

# 目录

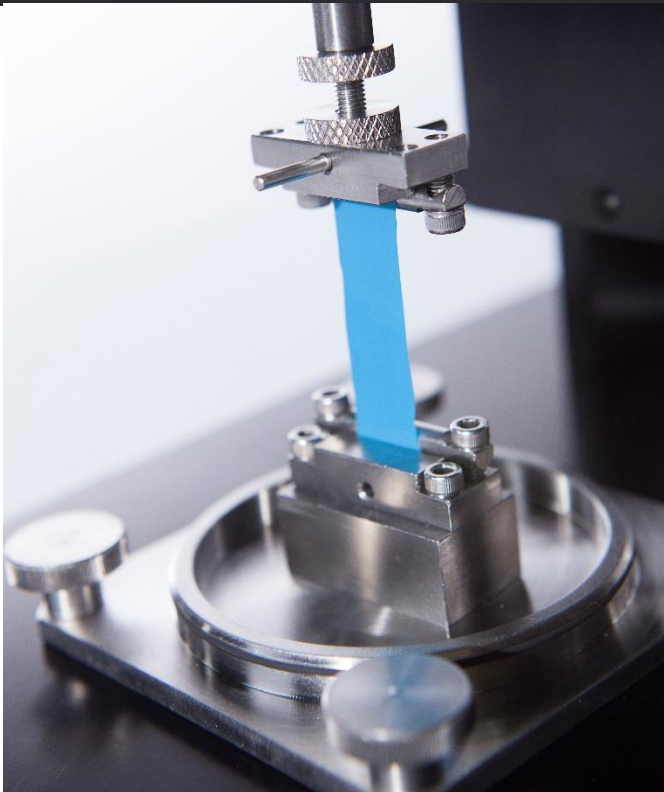
Benefits and Characteristics .....	6
Unique Features .....	8
Test Configurations Possibilities .....	9
Technical Specifications .....	10
Mechanical Testers .....	11
Model Mach-1 v500c .....	11
Model Mach-1 v500cs .....	12
Model Mach-1 v500ct .....	13
Model Mach-1 v500css .....	14
Model Mach-1 v500cst .....	15
Model Mach-1 v500csst .....	16
Educational Mach-1 .....	17
Stage Improvements .....	18
Load Cells .....	19
Indenters .....	23
Testing Chambers .....	24
Sample Holders.....	26
Manual Positionners .....	31
Others .....	32
Imaging .....	33
Software Add-On .....	34
Standard Operating Procedures .....	36
Case Studies .....	48

中国授权经销商  
世联博研（北京）科技有限公司-专注生物力学科研服务  
电话：010-67529703  
联系人:李先生，手机：18618101725



# COMPANY

Biomomentum manufactures and commercializes testing devices for the mechanical characterization of biomaterials and cartilage. The Mach-1™ multi-axial mechanical tester is the only all-in-one device designed for compression, tension, shear, friction, torsion and indentation mapping. The Mach-1™ is used in many university labs and is deemed an excellent educational tool.



Biomomentum also offers a full-service approach to biomechanical testing. In addition to performing highly controlled tests using a state-of-the-art technology, its expert team adheres to effective Standard Operating Procedures, develops reliable testing protocols, and delivers accurate data analysis reports in compliance with Good Laboratory Practice

# MECHANICAL TESTERS

Since 1999, our unique multiaxial mechanical tester has helped hundreds of scientists around the world to enhance and publish their innovative research activities related to biomaterials, tissues and soft materials.

The Mach-1™ multiaxial mechanical tester is the only all-in-one device designed for compression, tension, shear, friction, torsion and indentation mapping.



# TESTING SERVICES

Biomomentum is a service provider of high quality mechanical testing on biomaterials and tissues. Our worldwide clientele ranges from small medical device companies to well-established pharmaceutical firms. As experts in the field of biomedical engineering, we serve a multitude of industries while respecting the strict regulations that govern each business sector. Biomomentum offers a full-service approach to biomechanical testing.

In addition to performing highly controlled tests using our state-of-the-art technology, our expert team adheres to effective standard operating procedures, develops reliable testing protocols and delivers accurate data analysis reports in compliance with Good Laboratory Practice. As an extension of our services, we design and manufacture accessories tailored to meet our clients' specific study requirements. We collaborate with our clients and third-party CRO's to provide personalized testing solutions within a short time frame.

# BENEFITS AND CHARACTERISTICS

## Mach-1™

- Upgradable and adaptable to a large variety of materials and test configurations
- Compatible with a wide selection of uniaxial and multi-axial load cells
- Large selection of popular accessories & infinite possibility of custom-designed accessories
- Comes with a computer (Windows 10 Pro, Acquisition card, Webcam, etc.) and software (Mach-1 Motion & Mach-1 Analysis)
- User-friendly software for effective data collection and simplified analysis
- Accurately characterizes specimens with low mechanical properties or with dimensions falling within the micrometer to centimeter range
- Robust design; Will keep its integrity for years
- Excellent educational tool for students - Unlimited access to our lab modules
- Does not require lubrication or complex maintenance
- Occupies little laboratory space – Easy to lift for convenient re-location (fits within a standard culture incubator)
- Complemented by a team of scientific experts
- Performs uniaxial high-precision testing in compression and tension, in various modes including dynamic, static, and waveform loading
- No PID adjustment required to account for material properties
- Is the only device able to perform 3D normal indentation on a surface that is not flat
- Is used by renowned scientists
- Supported by a 24-month hardware warranty
- Free software upgrades within 2 years of purchase
- Online support and training of lab assistant included
- Data can be imported into third-party software for further analysis



# BENEFITS AND CHARACTERISTICS

## Testing services

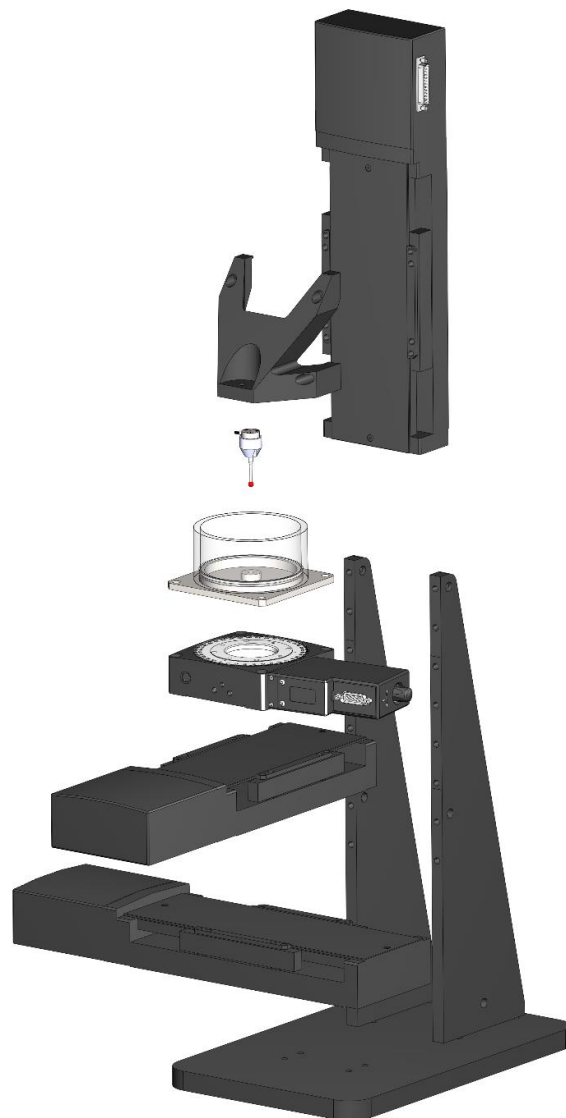
- Wide selection of tests
- Wide variety of materials to test: biological tissues, biomedical products and more
- Possibility to perform GLP compliant tests
- Personalized testing solutions within a short time frame
- Strong quality management system
- Proven expertise
- Full-service approach to biomechanical testing (study design, protocol development, conduct of the study, statistical analysis, quality assurance, etc.)
- Protocols and procedures (RMA) for the efficient shipping of samples (even from international locations)
- Team of experts who adheres to effective standard operating procedures
- Detailed procedures which ensures GLP-compliance of the testing services whenever required, in conformity with OECD Guidelines.
- Commitment to laboratory animal welfare; will take advantage of its cutting-edge technologies and innovative protocol designs to minimize the number of animals involved in a study.
- Commitment in helping you minimizing related costs; while making sure that, at the end, you will be able to support study's conclusions with the necessary statistical power. When insufficient preliminary data are available to determine the optimal sample size, we will suggest to run short a pilot study to maximize your chance of success.
- Strong Quality Management System which provides evidence of strict quality controls implemented to ensure product and service quality; (Complies with ISO 13485:2003, EN ISO 13485:2012 (Medical Devices), with FDA 21 CFR Part 820, with the European MDD 93/42/EEC and with the Canadian Medical Device Regulations 1998-783.)



# UNIQUE FEATURES

## Upgradable

The Mach-1™ has been designed to be easily upgraded with the addition of motorized stages, load cells and accessories, so it will evolve and constantly adapt to changes in your material research priorities.



## 3D Normal Indentation Mapping

Indentation usually requires the tested surfaces to be flat and it also requires the compression axis aligned perpendicularly to the articular surface. The 3D “Normal Indentation” function of the multi-axial mechanical tester Mach-1 v500css precisely detects the height and orientation of the surface at the XY position and records the load (multi-axial load cell) while simultaneously moving the three stages of the tester at different speeds to move a spherical indenter with a predefined displacement profile along a virtual axis normal to the surface of the sample.

# Test Configurations Possibilities

Due to its modular design, small footprint and numerous customization features, this top-of-the-line tester offers the versatility required in cutting edge biomaterial testing labs.

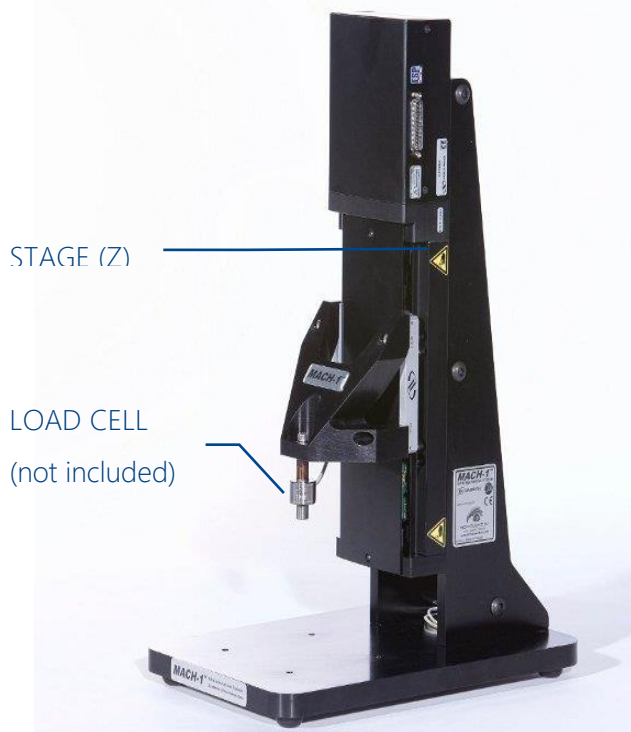
							
		v500c	v500cs	v500ct	v500css	v500cst	v500csst
Friction			✓	✓	✓	✓	✓
Shear			✓		✓	✓	✓
Torsion				✓		✓	✓
3D Profilometry					✓		✓
3D Normal Indentation					✓		✓
Tension		All testers					
Unconfined Compression		All testers					
Bending		All testers					
Puncture		All testers					
Indentation		All testers					
Positioning (XY Manual)		All testers					
Positioning (XY Auto)		Option					
Camera Feed		Option					
Dynamic Mechanical Analysis		Option					
Digital Image Correlation		Option					
Click <a href="#">HERE</a> to see all test configurations							

## Technical Specifications

The Mach-1™ has been designed to be easily upgraded with the addition of motorized stages, load cells and accessories, so it will evolve and adapt constantly to changes in your material research priorities.

						
	v500c	v500cs	v500ct	v500css	v500cst	v500csst
1 vertical stage (z)	✓	✓	✓	✓	✓	✓
1 horizontal stage (x)		✓		✓	✓	✓
1 horizontal stage (y)			✓	✓		✓
1 torsion stage (t)			✓		✓	✓
Width (mm)	230	405	230	405	405	405
Depth (mm)	350	350	350	495	350	495
Weight (excluding computer, controller and cable)	12.5 kg	17 kg	14.5 kg	21.5 kg	19 kg	23.5 kg
Travel range	100mm (Option: 50, 150, 200 or 250mm)					
Stage resolution	0.5µm (Option: 0.1µm)					
Max speed	50mm/s (Option: 100mm/s)					
Max acceleration	500mm/s <sup>2</sup>					
Height adjustable	490 – 685mm					
Acquisition rate	Adjustable 10 – 2500 Hz (all channels)					
Power input	100 – 240 V, 6.3 A, 50/60 Hz					
Computer included	Windows 10 Pro, Acquisition Card, Screen, HD Webcam (for effective and personalized technical support – if needed)					
Software included	Mach-1 Motion & Mach-1 Analysis					

# One vertical stage for various uniaxial testing



## Specifications

Motion Controller (# Axis)	1			
Stage Linear - Resolution	0.5 $\mu\text{m}$ (0.1 $\mu\text{m}$ in option)			
Computer Included?	Yes			
Acquisition rate	Adjustable from 10 to 2500 Hz (all channels)			
Stage	Vertical (Z)	Horizontal (X)	Horizontal (Y)	Rotation
	Yes	No	No	No
Dimensions	Width	Depth	Height	
	230 mm (9 in)	350 mm (14 in)	490 to 685 mm (19 to 27 in)	
Load Cell Included?	No			
Stage Linear – Travel Range	100 mm (50, 150, 200, 250 mm in option), Y is 50 mm			
Stage Linear – Max Speed	50 mm/s (100 mm/s in option)			
Stage Linear – Max Acceleration	500 mm/s <sup>2</sup>			
Power Input	100-240 V, 6.3 A, 50/60 Hz			
Software Included?	Yes, Mach-1 Motion and Mach-1 Analysis			
Computer (Min. Spec.)	Intel Core I5, 4GB 1600 MHz, Windows 10 Pro, Acquisition Card, 22" Flat Screen, HD Webcam, Sound bar, keyboard and mouse.			
Weight	12.5 kg			



One vertical stage and one horizontal stages for compression, tension and shear testing

### Specifications

Motion Controller (# Axis)	2			
Stage Linear - Resolution	0.5 $\mu\text{m}$ (0.1 $\mu\text{m}$ in option)			
Computer Included?	Yes			
Acquisition rate	Adjustable from 10 to 2500 Hz (all channels)			
Stage	Vertical (Z)	Horizontal (X)	Horizontal (Y)	Rotation
	Yes	Yes	No	No
Dimensions	Width	Depth	Height	
	405 mm (16 in)	350 mm (14 in)	490 to 685 mm (19 to 27 in)	
Load Cell Included?	No			
Stage Linear – Travel Range	100 mm (50, 150, 200, 250 mm in option), Y is 50 mm			
Stage Linear – Max Speed	50 mm/s (100 mm/s in option)			
Stage Linear – Max Acceleration	500 mm/s <sup>2</sup>			
Power Input	100-240 V, 6.3 A, 50/60 Hz			
Software Included?	Yes, Mach-1 Motion and Mach-1 Analysis			
Computer (Min. Spec.)	Intel Core I5, 4GB 1600 MHz, Windows 10 Pro, Acquisition Card, 22" Flat Screen, HD Webcam, Sound bar, keyboard and mouse.			
Weight	17 kg			

# One vertical and one rotation stages for compression, tension and shear testing

STAGE (Z)

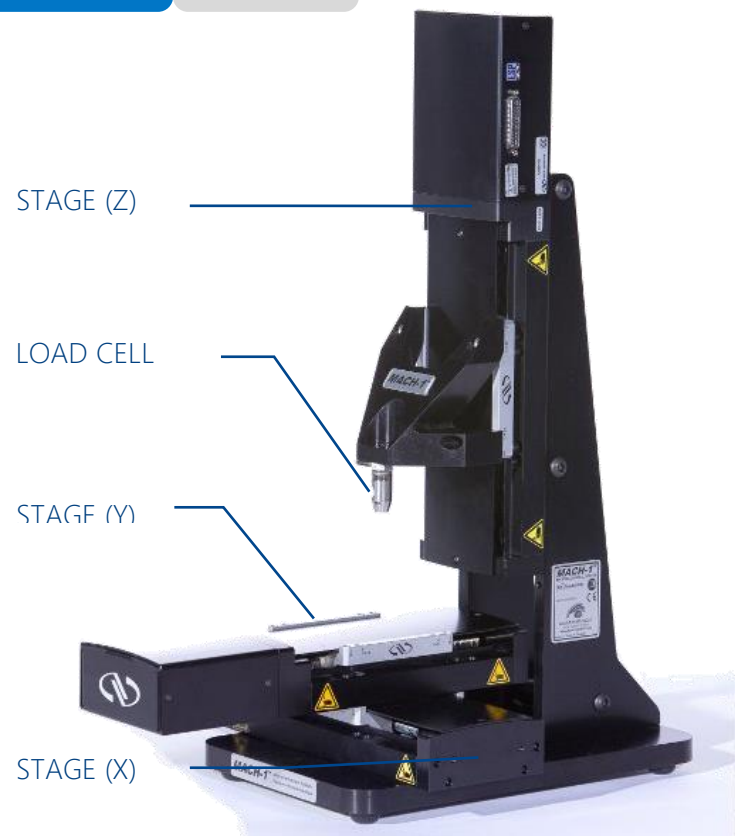
LOAD CELL  
(not included)ROTATION  
STAGE

PRODUCTS

## Specifications

Motion Controller (# Axis)	2			
Stage Linear - Resolution	0.5 $\mu\text{m}$ (0.1 $\mu\text{m}$ in option)			
Stage Rotational - Resolution	0.5 $\text{m}^\circ$			
Computer Included?	Yes			
Acquisition rate	Adjustable from 10 to 2500 Hz (all channels)			
Stage	Vertical (Z)	Horizontal (X)	Horizontal (Y)	Rotation
	Yes	No	No	Yes
Dimensions	Width	Depth	Height	
	230 mm (9 in)	350 mm (14 in)	490 to 685 mm (19 to 27 in)	
Load Cell Included?	No			
Stage Linear – Travel Range	100 mm (50, 150, 200, 250 mm in option), Y is 50 mm			
Stage Linear – Max Speed	50 mm/s (100 mm/s in option)			
Stage Linear – Max Acceleration	500 $\text{mm/s}^2$			
Stage Rotational - Travel Range	$\pm$ Infinite			
Stage Rotational - Max Speed	80 $^\circ/\text{s}$			
Stage Rotational - Max Acceleration	320 $^\circ/\text{s}^2$			
Power Input	100-240 V, 6.3 A, 50/60 Hz			
Software Included?	Yes, Mach-1 Motion and Mach-1 Analysis			
Computer (Min. Spec.)	Intel Core I5, 4GB 1600 MHz, Windows 10 Pro, Acquisition Card, 22" Flat Screen, HD Webcam, Sound bar, keyboard and mouse.			
Weight	14.5 kg			

One vertical and two horizontal stages for compression, tension and shear testing (multi-axial configuration)



### Specifications

Motion Controller (# Axis)

3

Stage Linear - Resolution

0.5  $\mu\text{m}$  (0.1  $\mu\text{m}$  in option)

Computer Included?

Yes

Acquisition rate

Adjustable from 10 to 2500 Hz (all channels)

Stage	Vertical (Z)	Horizontal (X)	Horizontal (Y)	Rotation
	Yes	Yes	Yes	No

Dimensions	Width	Depth	Height
	405 mm (16 in)	495 mm (14 in)	490 to 685 mm (19 to 27 in)

Load Cell Included?

No

Stage Linear – Travel Range

100 mm (50, 150, 200, 250 mm in option), Y is 50 mm

Stage Linear – Max Speed

50 mm/s (100 mm/s in option)

Stage Linear – Max Acceleration

500 mm/s<sup>2</sup>

Power Input

100-240 V, 6.3 A, 50/60 Hz

Software Included?

Yes, Mach-1 Motion and Mach-1 Analysis

Computer (Min. Spec.)

Intel Core I5, 4GB 1600 MHz, Windows 10 Pro, Acquisition Card, 22" Flat Screen, HD Webcam, Sound bar, keyboard and mouse.

Weight

21.5 kg

# One vertical, one horizontal and one rotation stages for compression, tension and shear testing (multi-axial configuration)

STAGE (Z)

LOAD CELL  
(not included)

ROTATION  
STAGE

STAGE (X)



PRODUCTS

## Specifications

Motion Controller (# Axis)	3			
Stage Linear - Resolution	0.5 $\mu\text{m}$ (0.1 $\mu\text{m}$ in option)			
Stage Rotational - Resolution	0.5 $\text{m}^\circ$			
Computer Included?	Yes			
Acquisition rate	Adjustable from 10 to 2500 Hz (all channels)			
Stage	Vertical (Z)	Horizontal (X)	Horizontal (Y)	Rotation
	Yes	Yes	No	Yes
Dimensions	Width	Depth	Height	
	405 mm (16 in)	350 mm (14 in)	490 to 685 mm (19 to 27 in)	
Load Cell Included?	No			
Stage Linear – Travel Range	100 mm (50, 150, 200, 250 mm in option), Y is 50 mm			
Stage Linear – Max Speed	50 mm/s (100 mm/s in option)			
Stage Linear – Max Acceleration	500 $\text{mm/s}^2$			
Stage Rotational - Travel Range	$\pm$ Infinite			
Stage Rotational - Max Speed	80 $^\circ/\text{s}$			
Stage Rotational - Max Acceleration	320 $^\circ/\text{s}^2$			
Power Input	100-240 V, 6.3 A, 50/60 Hz			
Software Included?	Yes, Mach-1 Motion and Mach-1 Analysis			
Computer (Min. Spec.)	Intel Core I5, 4GB 1600 MHz, Windows 10 Pro, Acquisition Card, 22" Flat Screen, HD Webcam, Sound bar, keyboard and mouse.			
Weight	19 kg			

One vertical, two horizontal and one rotation stage for compression, tension, shear and torsion testing (multi-axial configuration)

STAGE (Z)

LOAD CELL

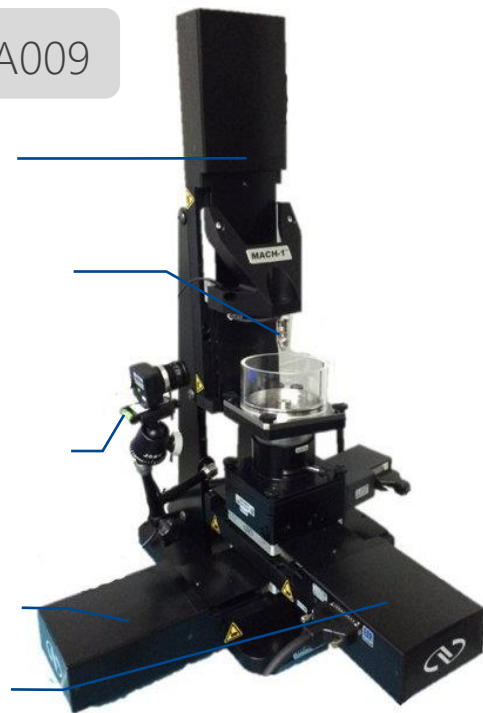
(Not included)

CAMERA

(Not included)

STAGE (X)

STAGE (Y)



PRODUCTS

### Specifications

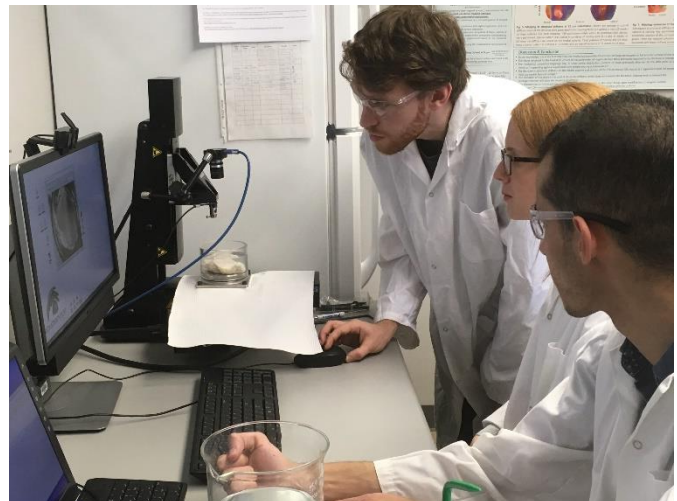
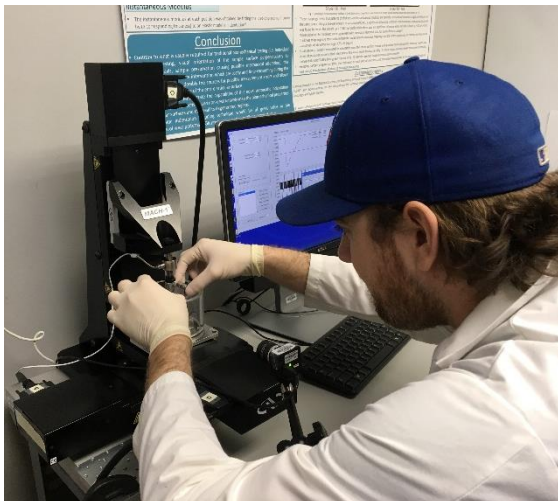
Motion Controller (# Axis)	3			
Stage Linear - Resolution	0.5 $\mu\text{m}$ (0.1 $\mu\text{m}$ in option)			
Stage Rotational - Resolution	0.5 $\text{m}^\circ$			
Computer Included?	Yes			
Acquisition rate	Adjustable from 10 to 2500 Hz (all channels)			
Stage	Vertical (Z)	Horizontal (X)	Horizontal (Y)	Rotation
	Yes	Yes	Yes	Yes
Dimensions	Width	Depth	Height	
	405 mm (16 in)	495 mm (19.5 in)	490 to 685 mm (19 to 27 in)	
Load Cell Included?	No			
Stage Linear – Travel Range	100 mm (50, 150, 200, 250 mm in option), Y is 50 mm			
Stage Linear – Max Speed	50 mm/s (100 mm/s in option)			
Stage Linear – Max Acceleration	500 mm/s <sup>2</sup>			
Stage Rotational - Travel Range	$\pm$ Infinite			
Stage Rotational - Max Speed	80 $^\circ/\text{s}$			
Stage Rotational - Max Acceleration	320 $^\circ/\text{s}^2$			
Power Input	100-240 V, 6.3 A, 50/60 Hz			
Software Included?	Yes, Mach-1 Motion and Mach-1 Analysis			
Computer (Min. Spec.)	Intel Core I5, 4GB 1600 MHz, Windows 10 Pro, Acquisition Card, 22" Flat Screen, HD Webcam, Sound bar, keyboard and mouse.			
Weight	23.5 kg			

## Educational Mechanical Tester Model Mach-1 v500c with undergraduate lab

Our undergraduate educational package can be customized with a wide selection of tester configurations, accessories and lab modules from our catalog. You can make your own educational package based on your budget and teaching objectives! The basic educational package is a turn-key solution.

### Included Items

- |   |       |
|---|-------|
| • Mechanical tester   | MA001 |
| • Single-axis load cell (100N)  | MA296 |
| • 3 Lab modules   |       |
| ○ Unconfined compression of hydrogel disk   | MA300 |
| ○ Tension and rupture of skin   | MA301 |
| ○ Bending of bone   | MA302 |
| • Detailed procedure for sample preparation, mechanical testing and data analysis, descriptive video capsule and wrap-up questions. |       |
| • Testing Chamber   | MA626 |
| • Spherical indenter  | MA679 |
| • Flat indenter   | MA262 |
| • Small chamber   | MA740 |
| • 3-point bending fixture   | MA097 |



### Replacement of a motorized linear stage with one of better resolution or modified travel

When your quotation contains at least one linear motorized stage, you can add these items to replace it with one of better resolution or modified travel range. For better resolution, the stage resolution will be improved from 0.5 to 0.1  $\mu\text{m}$ . The improved stage has also better driving motor and encoding method improving overall performances (accuracy 0.8 to 0.6  $\mu\text{m}$ , repeatability bi-directional  $\pm 0.4$  to  $\pm 0.1$   $\mu\text{m}$ , repeatability origin  $\pm 0.5$  to  $\pm 0.1$   $\mu\text{m}$ , max speed 50 to 100 mm/s). The overall stage length is also increased by 34 mm in the motor head section.

Resolution Improved to 0.1  $\mu\text{m}$  on a 50 mm Stage

MA174

---

Resolution Improved to 0.1  $\mu\text{m}$  on a 100 mm Stage

MA175

Stage Linear - Max Speed, 100 mm/s

Stage Linear - Resolution, 0.1  $\mu\text{m}$

---

Travel Range decreased to 50 mm on a Stage

MA176

Stage Linear - Travel Range, 50 mm

---

Travel Range Increased to 150 mm on a Stage

MA177

Stage Linear - Travel Range, 150 mm

---

Travel Range Increased to 200 mm on a Stage

MA178

Stage Linear - Travel Range, 200 mm

---

Travel Range Increased to 250 mm on a Stage

MA179

Stage Linear - Travel Range, 250 mm



A single-axis load cell can measure the force applied axially on the Z axis, either in tension or in compression. It can be used for indentation, tension, bending and compression testing.

Single-Axis Load Cell (100 N) with amplification module  
MA296

Single-Axis Load Cell (250 N) with amplification module  
MA297

Single-Axis Load Cell (10 N) with amplification module  
MA410

Single-Axis Load Cell (0.5 N) with amplification module  
MA996

Single-Axis Load Cell (1.5 N) with amplification module  
MA999



ACCESSORIES

Specifications					
	MA297	MA296	MA410	MA999	MA996
Force Ranges (N)	250	100	10	1.5	0.5
Force Resolutions (mN)	12.5	5	0.5	0.075	0.025
Upper Attachment	1/4-28 (Female Thread)				
Lower Attachment	1/4-28 (Female Thread)				
Linearity	+/- 0.15% Full Scale				
Required accessories	MA337	MA337	MA337	MA336	MA336

A multiple-axis load cell can measure forces and torques on 3 different axes at the same time. This allows the user to measure all force components in tension/compression, shear and torsion test configurations. An adapter for the attachment of the calibration weight and indenters/grips is screwed underneath the load cell.

Multiple-Axis Load Cell (17 N) with amplification module  
MA233

Multiple-Axis Load Cell (35 N) with amplification module  
MA234

Multiple-Axis Load Cell (70 N) with amplification module  
MA235

Maximum allowable single-axis overload values are 3.1 to 13.8 times rated capacities.



Multiple-Axis Load Cell (250 N) with amplification module  
MA236

It should be noted that the maximum axial load that the tester can generate is 250N. Applying moments beyond  $\pm 30$  lb-in ( $\pm 3.4$  Nm) in  $T_z$  can cause permanent damage to the load cell. Maximum allowable single-axis overload values are 7.1 to 15.1 times rated capacities.

Specifications					
		MA233	MA234	MA235	MA236
Ranges	Vertical Axis (N)	17	35	70	250
	Horizontal Axis (N)	12	25	50	250
	Torsion Axis (N.mm)	120	250	500	3000
Resolution	Vertical Axis (mN)	0.85	1.75	3.5	12.5
	Horizontal Axis (mN)	0.6	1.25	2.5	12.5
	Torsion Axis (N.mm)	0.006	0.0125	0.025	0.15
Upper Attachment		3 x M2 (Female Thread, max L=3.5 mm)			
Lower Attachment		1/4-28 (Female Thread)			
Linearity		$\leq 2\%$ Full Scale (Each Channel)			
Required Accessories		MA336, MA721	MA337, MA721	MA337, MA721	MA337, MA721

## Extends the calibration range of a Multiple-Axis Load

An additional calibration enables a new load range for a multiple-axis load cell. This additional calibration consists in a new amplification module in which you can connect your multiple-axis load cell. Only one calibration can be active at a time, but the load cell can freely be swapped between any available amplification module. This module is calibrated for the lowest load range available, making it ideal for lower forces and torques requiring higher precision.

Additional Calibration (17 N) and amplification module for the Multiple-Axis Load Cell  
MA239

---

Additional Calibration (70 N) and amplification module for a Multiple-Axis Load Cell  
MA240

---

Additional Calibration (35N) and amplification module for a Multiple-Axis Load Cell  
MA241

A calibration weight to verify the integrity of a load cell

These calibration weights are used at the beginning of each test session to verify the integrity of a load cell.



Calibration Weight 100 g

MA336

Material: Stainless Steel 304

Weight: 100 g (Approx.)

Upper Attachment: 1/4-28 male thread



Calibration Weight 500 g

MA337

Material: Stainless Steel 304

Weight: 500 g (Approx.)

Upper Attachment: 1/4-28 male thread

## Flat Indenter

D = 2 mm (MA685)

D = 3 mm (MA686)

D = 4 mm (MA687)

D = 12.5 mm (MA262)

D = 25 mm (MA678)

---

## Spherical Indenter

D = 1 mm (MA680)

D = 6.35 mm (MA679)

---

## Kit of Spherical Indenters - Ruby balls,

D = 0.3(2X), 0.5(2X), 1, 2, 5 mm (MA030)

---

## Quick Connection Adapter (incl. 3 Dowel Pin)

D = 3.2 mm (MA670)

---

## Hardness indenters

Indenter Berkovich- MA683

Indentation depth = 20 $\mu$ m

Indenter Vickers- MA684

Indentation depth = 20 $\mu$ m

---

## Kit of Needles

MA690

Normally used for thickness measurement.





Electromechanical Testing Chamber

MA070

This chamber has been designed for the synchronized measurement of electric potential distribution during compression of an electromechanically active material (e.g. connective tissues, charged hydrogel, etc.). This chamber presents 5 differential Ag-AgCl electrode channels and a larger reference electrode. The chamber can be filled with PBS solution.



Multi-Well Plate Holder

MA555

This item has been designed to firmly hold in place a multiwell plate on the tester. Any type of multiwell plate fitting the Corning® Costar® footprint can be fitted on the plate.



Chamber (D = 98 mm), 2 Walls  
(50.8 and 76.2 mm) for Holders

MA626

This testing chamber is a center piece of the Mach-1 mechanical tester. The threaded base allows the user to fit a multitude of accessories helping to fix the sample. The sealed transparent walls allow the user to perform tests on submerged samples. This test chamber can be in contact with saline water without risk of oxidation. It comes with two swappable walls of 50.8 and 76.2 mm of height.



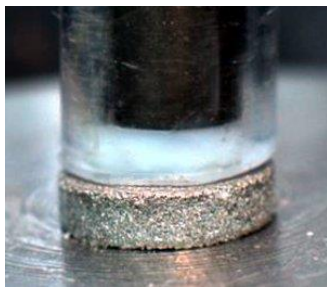
Chamber (60 mL) with 3 Portholes  
for Small Samples  
MA635

This testing chamber has been designed for the testing of small sample. This chamber has been optimized with three orthogonal clear portholes to facilitate imaging of the sample from the side. One wall presents no porthole to provide a black background for imaging.



Sample Holder and Chamber, Flat  
with Wall (D = 37 mm) for MA626  
MA740

This small testing chamber is particularly useful to conduct unconfined compression test. A transparent wall can be slid over to create a container for a bathing solution. Using this small wall instead of the large wall of MA626 will considerably reduce the volume of bathing solution required to cover the sample.



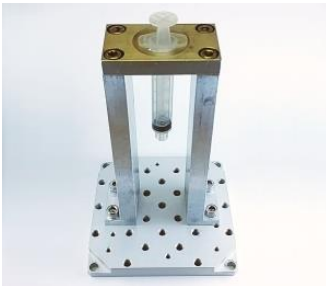
Confined Compression Chamber Kit,  
for MA626  
MA742

Confined compression testing measures the capacity of the material to withstand axial compressive loads without expanding perpendicularly to the force. Confined compression tests are usually performed on biphasic materials (e.g. poroelastic materials). The disk-shaped sample is compressed by a sliding piston and the liquid phase can be expelled through a porous disk (2  $\mu\text{m}$  pore size). A magnet, installed on the piston facilitates its use and installation.



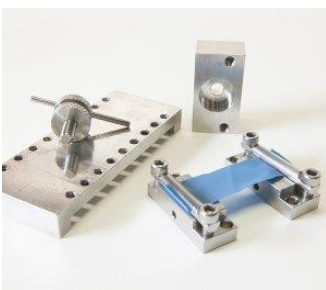
Sample Holder, Osteochondral Core -  
for MA626  
MA080

It has been designed to attach an osteochondral core (a cylindrical sample made of a cartilage layer over the underlying bone) to the base of the testing chamber (MA626). The cartilage layer can be tested under unconfined compression. This configuration is not exactly an unconfined compression configuration (since the bottom surface is attached on the bone), however, since the sample maintains its shape leads to more reproducible results. A manual angular stage is highly recommended to visually orient the cartilage surface perpendicularly with the compression axis. This holder can also be used to maintain other types of small samples in place (e.g. small bones, fibers, small tendons, etc.).



Sample Holder, Syringe Holder Kit  
MA085

This syringe holder is used to measure the expression or aspiration force. It is designed to be compatible with syringes of various sizes. Perforated disks placed on top of the holder allow switching between syringes of different sizes. Under expulsion testing, the syringe piston is pushed by the vertical stage under the load cell to evaluate the performance of the assembly for a particular solution.



Sample Holder, Tensile Grip (2 Sets)  
with Sample-Mounting Plate  
MA090

This sample holder includes two pairs of grips used for tensile tests with a mounting plate allowing easy sample setup. These grips were designed for tension testing of soft sheet material. Their C-shaped cavities, coupled with the screwed stainless-steel bar, solidly lock the sample in the grip. This set includes 4 grips (2 sets of 2) and the mounting plate allowing an easy fixing of the sample.



Sample Holder, T-shaped Tensile  
Fixtures (D=0.8 mm)  
MA092

Originally developed for the mechanical evaluation of rat aorta sections, this pair of grips can be used for tension testing of miniature samples shaped as a tube or ring. Each T-shaped support comes attached in a quick connection adapter. One is secured at the bottom of the chamber and the second one is placed upside down under the load cell. After alignment of both supports along the vertical axis of the tester, the small ring of material (e.g. a vein, artery, ring of hydrogel, etc.) is slid over both top and bottom posts prior to tension testing.



Sample Holder, Torsion on Rodent  
Long Bone  
MA096

This holder allows for an easy installation and fixture of the bone sample. It is designed to assure the crucial alignment of the sample with the torsion axis.



Sample Holder, 3 Point Bending

Fixture

MA097

This set of holders has been designed for 3-point bending tests. The base is equipped with two supporting pin holders. These pin holders can easily be moved to the desired spacing thanks to the integrated ruler on the base. The top mount is the loading pin holder. It is fixed to the load cell and secured in place with a locking pin.

Force Range (Fz): Up to 2.5 kN (tester max force is 250N)



Lap Shear Test Fixtures

MA133

An important property to test in adhesive testing is the resistance to shear force along the bonded interfaces. Based on fixtures designed for strong bonding in hard plastic and metallic part, these fixtures have been optimized for the testing of the bonding properties between biomaterials or tissues. It comes with a special holder designed to facilitate the in-situ preparation of hydrogels directly injected between the two platens to minimize exposure to air. In the context of hydrogels, shear strength and its adherence properties with the platen material can be tested.



Sample Holder, Flat with Screw  
Clearances (D = 85 mm) - for

MA626

MA610

This sample holder consists of a round plate with screw clearances. It is threaded to fit on MA626 test chamber. The sample holder has been designed to secure in place an entire articular surface during 3D mechanical or thickness mapping protocol. The flat bony surface is secured in place on the plate using wood screws passing through clearance holes from the bottom side of the plate.



Glue Loctite® 4013™ Prism®

MA634

LOCTITE® 4013 Prism medium viscosity, one-part room temperature cure, instant adhesive designed to provide fast fixturing on thermoplastic, thermoset plastic and metal. Suitable for use in the assembly of disposable medical devices. ISO-10993 Biological Tested for medical device use.



Sample Holder, 6-Screw (D = 63.5 mm) with Cone-Ended Screws for

MA626

MA646

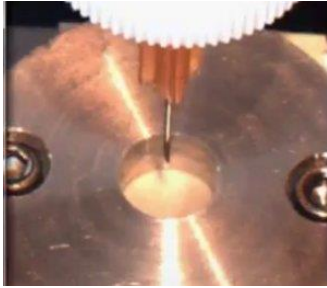
This sample holder consists of a round plate with six screws allowing to hold the sample in place by the side. It has been designed to hold irregular block sample with a flat base. Two sets of six screws allow samples with critical dimension from 7.5 to 63.5 mm to be tightly held in place without altering their properties by applying excessive side pressure. The holder is threaded to fit on the testing chamber (MA626) and has knurled diamond side surface allowing easy installation.



Tack Testing Fixtures

MA734

This sample holder is used to measure the tackiness (instant adhesion) of an adhesive layer or tape. These tack testing fixtures can be used to measure the tack properties (instantaneous adhesion) of adhesives either through the inverted probe (ASTM D2979) or the loop (ASTM D6195) tack testing methods. It comprises: for the inverted probe technique (a flat indenter with a 5-mm diameter and annular loading weights) and for the loop (a tensile grip and a 1 inch flat base). The force required to completely peel out the material provides its tackiness.



Holder for Puncture Test

MA735

This accessory is designed to maintain in place a sheet of material during puncture. It allows proper clamping of the sheet material to maintain it straight and horizontal position during a penetration test.



Compliance Ball

MA745

This accessory is used to measure the tester compliance in 3D. The compliance of the tester (or the reciprocal of the stiffness) is the deformation observed in the tester overall structure for a certain level of force. All mechanical testers present a certain level of compliance that the manufacturer tries to minimize and that is generally negligible regarding the compliance of the sample. For multiaxial tester, ensuring low compliance on all axis is more challenging. This compliance ball is made of hard metal, presents a high degree of sphericity and is screwed onto the testing chamber base at the location of the sample. After setting the tester in the same configuration (actuators stacking and position on the frame), installation of the multiaxial load cell and the desired spherical indenter, the ball is mapped at various positions with the normal indentation function. Assuming that this rigid ball has a known and limited deformation for the indentation force applied, the outcome of the normal indentation can be used to map the 3D compliance of the tester. The outcome of this testing can be used to compensate 3D stiffness mapping of stiff samples.

# Manual Positioners

These manual displacement stages allow the manual positioning of the sample under the compression axis in various directions.

X Positioner (50 mm) with Manual Adjustment Screw

MA761

X Positioner (50 mm) with Manual Vernier Micrometer

MA763

XY Positioner (100 mm) with Manual Adjustment Screws

MA765

XY Positioner (50 mm) with Manual Vernier Micrometers

MA767

Angular Positioner (Tilt:  $\pm 25^\circ$ , Rotation:  $360^\circ$ ) Manual

MA775



Angular Positioner  
MA775

ACCESSORIES

## Specifications

	MA761	MA763	MA765	MA767	MA775
Manual Positioning Axis	One horizontal axis	One horizontal axis	One horizontal axis	Two orthogonal horizontal axes	Surface perpendicularly to the compression axis
Sensitivity ( $\mu\text{m}$ )	3.5	1	3.5	1	-
Travel Range	50 mm	50 mm	100 mm (X), 100 mm (Y)	50 mm (X), 50 mm (Y)	$\pm 25^\circ$ (Tilt from horizontal), $360^\circ$ (Rotation)



Dogbone Sample Cutting Die  
MA333

Cutting die for tension testing on tissues and biomaterials. Dogbone-shaped samples are usually prepared for tensile testing. This shape will minimize the risk of failure inside the grips and make the tensile stress concentrate in the gauge section. This cutting die kit are in fact very sharp razor blade spacers used to create a controlled width in the gauge section of the sample. Remaining shape is then created manually using a scalpel.



Computer Upgrade  
MA444

This item provides you with a computer system with improved specifications. Add this item to your cart to replace the basic computer system included in the mechanical tester package with one showing improved specifications.

Height: 2.76 in

Width: 5.7 in

Depth: 9.8 in

Computer (Min. Spec.): SlimPro SP685EP Mini PC RAM (16GB), Intel® Core™ i5, Solid State Disk (480GB)



Macro Zoom (10X) Lens with Stand  
and Lighting  
MA730

This item allows to reach high resolution images of small samples (under 3 mm). Min diagonal FOV: 7.3 mm



Microscope Lens (8X)  
MA731

Allow to reach high resolution images of small samples (under 4 mm).  
Min diagonal FOV: 0.6 mm



Color Camera (1.3MPx) with Lens  
(12.5mm) and Support  
MA732

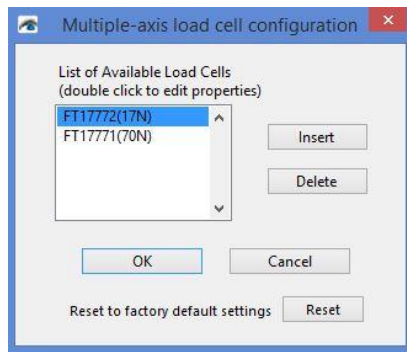
The color camera can be used to image the samples for further analysis.



Mach-1 Motion Software - Add-On  
for Camera Feed  
MA723



A Camera Feed can be added to the Mach-1 mechanical Tester. The live video streaming facilitates the setup of test sequences, particularly for small samples. This feature allows the capture of series of high definition images of the sample during mechanical testing. Image capture is synchronized with the raw data of the mechanical test. These images can be easily exported to third-party software for image processing. For example, they can be exported to Matlab® for deformation field analysis.



This software add-on is required to activate multiaxial load cell

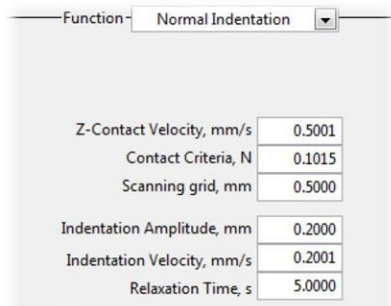
Mach-1 Motion Software - Add-On  
for Multiple-Axis Load Cell  
MA721

“Analog Inputs” Window



Adds analog inputs to the tester. For each channel the ground reference setting can be set to “Differential” or “Single-Ended” and the voltage range set to  $\pm 10V$ ,  $\pm 5V$ ,  $\pm 1V$  or  $\pm 0.2V$ . Signals shall be connected to the dedicated SCC-68 box that is provided to users with this software add-on. See the SCC-68 reference label inside the box and/or the SCC-68 user guide for the proper location of the inputs terminals.

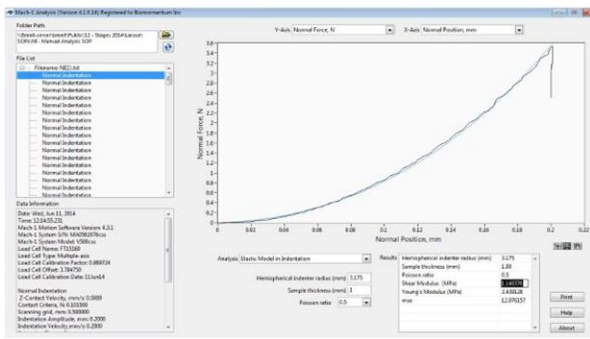
Mach-1 Motion Software - Add-On  
for Analog Inputs  
MA721



“Normal Indentation” Parameters

Activates the Normal Indentation Function. This function precisely detects the height and orientation of the surface at the XY position and records the load (for multiaxial load cell only) while simultaneously moving the three linear stages at different speeds to move a spherical indenter with a predefined displacement profile along a virtual axis normal to the surface of the sample.

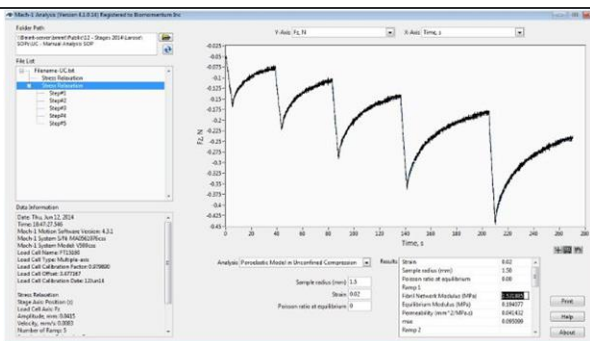
Mach-1 Motion Software - Add-On  
for Normal Indentation  
MA724



Mach-1 Analysis Software - Add-On for Indentation Testing (Elastic Model)

MA725

This tool allows for the computing and visualizing of the shear modulus (MPa) and the Young's modulus (MPa) from an indentation test performed using a spherical indenter. This model is well adapted for the mechanical description of samples bounded on a flat rigid support, for example: any sheet of material lying on a rigid chamber base or a cartilage layer attached to a thick subchondral bone. A user license is required to obtain the results of the elastic model in indentation. Results analysis is performed considering the indentation mechanics of an infinitely wide elastic layer bonded to a rigid half-space which has been developed as a model for the layered geometry of cartilage and subchondral bone (Hayes et al., 1972).

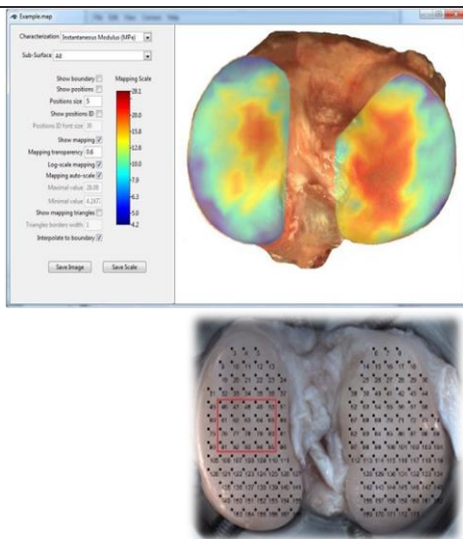


Mach-1 Analysis Software - Add-On for Unconfined & Confined Compression (Poroelastic Model)

MA726

This tool allows for the computing and visualizing of the aggregate modulus (MPa), the permeability ( $\text{mm}^2/\text{MPa}\cdot\text{s}$ ) and the mean square error (MSE) of the fit calculated from a "Stress Relaxation" curve (load or force vs. time) in confined compression on a disk sample. The curve is fitted to the linear biphasic model (Mow et al., 1980 or Bursać et al., 1999) in order to obtain the mechanical properties of the disk. This model is a well adapted model for the mechanical description of biphasic samples, for example: cartilage or gel samples. A user license is required to obtain the results of the poroelastic model in confined compression.

ACCESSORIES



The Mapping Toolbox is a data management software designed to record, manage, analyze and display various types of local characterization performed on the surface of a sample. Characterization data is handled in the form of maps overlaid onto a representative image of the sample surface. Equipped with a camera, the software can also be used as a camera-registration positioning system to capture image of the sample surface and to facilitate manual characterization mapping. This software can manage various types of quantitative value data to create mappings of e.g. stiffness, thickness, chemical content, density, temperature, image path, etc. Eventually, new statistical modules will be released to perform various statistical analyses with a single or multiple characterization mappings.

Mapping Toolbox for a Cartographic Characterization of Data

MT337

# Standard Operating Procedures



# AUTOMATED INDENTATION MAPPING

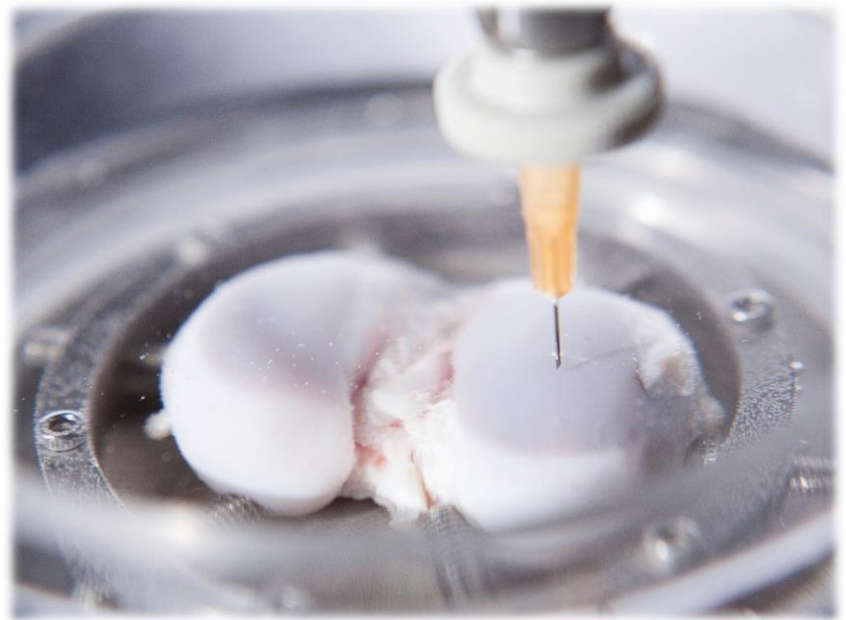
## Purpose

This procedure describes a standard method to realize an automated indentation mapping over the surface of a sample using the Mach-1™ mechanical tester (model v500css, with software add-on for Automated Indentation Mapping). Analysis of the measurement results is part of a companion document (SW186-SOP01-D)

## Scope

This procedure can be used for the *ex vivo* automated indentation mapping over the surface of a sample. Sample's dimension and mechanical properties must be compatible with the Mach-1™ configuration and must allow proper attachment in the testing chamber. It is highly recommended to use standard protocol for sample preparation to facilitate positioning in the chamber and facilitate eventual comparison between samples. Some mapping parameters must be specified in an associated protocol: filename, sample holder type, mapping dimensioning method, surface positioning template (if applicable), position grid (#columns X # rows), multiple-axis load cell type, spherical indenter type and normal indentation function parameters.

# AUTOMATED THICKNESS MAPPING OF AN ARTICULAR SURFACE

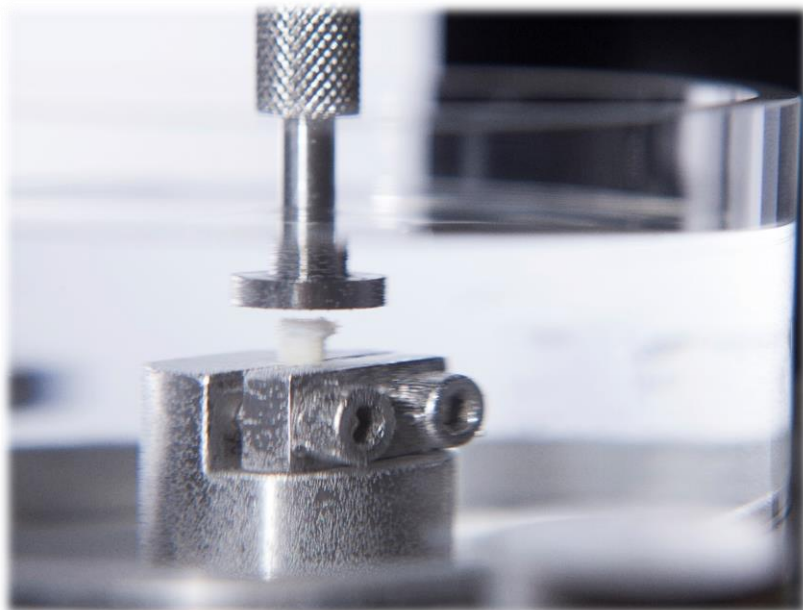


## Purpose

This procedure describes a standard method to realize an automated thickness mapping over the non-planar surface of articular cartilage using the Mach-1™ mechanical tester (model v500css, with software add-on for Automated Thickness Mapping). Analysis of the measurement results is part of a companion document (SW186-SOP02-D)

## Scope

This procedure can be used for the *ex vivo* automated thickness mapping over non-planar surface of articular cartilage. Sample's dimension and mechanical properties must be compatible with the Mach-1™ configuration and must allow proper attachment in the testing chamber. It is highly recommended to use standard protocol for sample preparation to facilitate positioning in the chamber and facilitate eventual comparison between samples. Some mapping parameters must be specified in an associated protocol: filename, sample holder type, mapping dimensioning method, surface positioning template (if applicable), position grid (#columns X # rows), multiple-axis load cell type, needle probe type and Find Contact function parameters.



## UNCONFINED COMPRESSION OF AN ARTICULAR CARTILAGE OSTEOCHONDRAL CORE

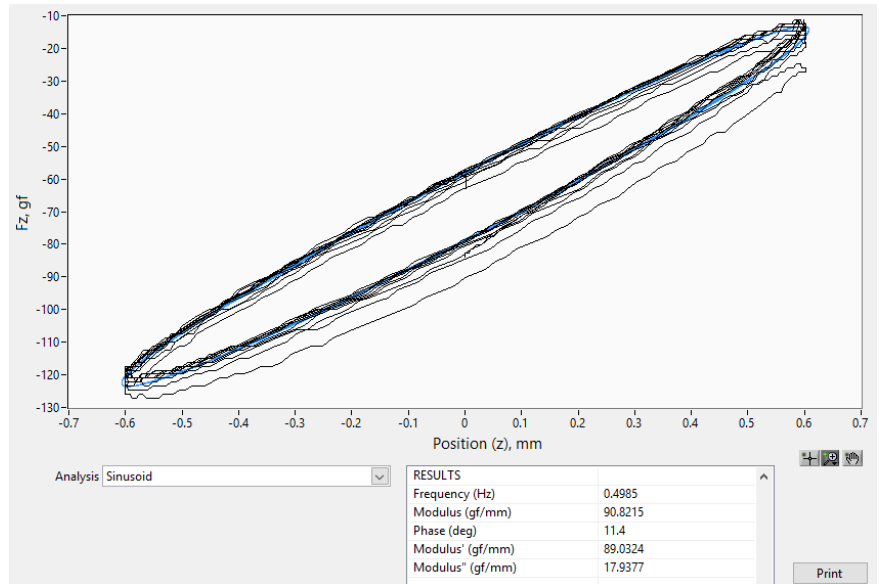
### Purpose

This procedure describes a standard method to realize unconfined compression on an osteochondral core using the Mach-1™ mechanical tester. Analysis of the measurement results is part of a companion document (SW186-SOP03-D)

### Scope

This procedure can be used for the *ex vivo* unconfined compression on an osteochondral core. It is highly recommended to use standard protocol for sample preparation to facilitate positioning in the chamber. Some mapping parameters must be specified in an associated protocol: filename, vertical stage resolution, load cell type, flat indenter type, cartilage layer thickness and stress-relaxation parameters.

# DYNAMIC MECHANICAL TESTING

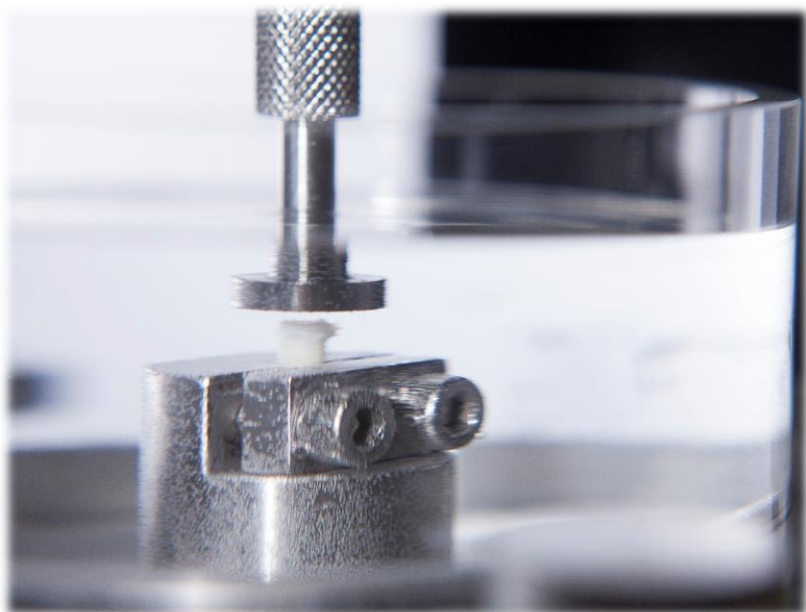


## Purpose

This document describes a standard method to assess the frequency behavior of the dynamic mechanical properties of material through the complex Young' s ( $E^*$ ) or shear ( $G^*$ ) modulus using the Mach-1™ mechanical tester. Analysis of the measurement results is part of a companion document (SW186-SOP04-D)

## Scope

This method can be applied on any type of material if the sample's shape and dimension are compatible with the specifications presented in the material section and that the involved displacements, strain rates, forces or torques remain within tester specifications.



# UNCONFINED COMPRESSION OF A DISK

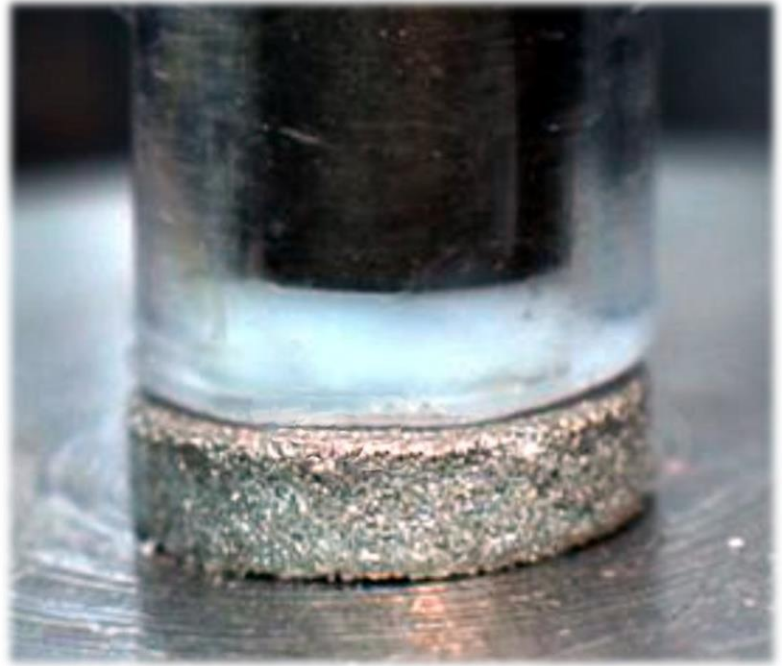
## Purpose

This procedure describes a standard method to realize unconfined compression on a disk-shaped sample using the Mach-1™ mechanical tester. Complementary reference is part of a mandatory companion document (MA056-SOP03-D).

## Scope

This procedure can be used for the *ex vivo* unconfined compression on a disk-shaped sample. It is highly recommended to use standard protocol for sample. Some mapping parameters must be specified in an associated protocol: filename, vertical stage resolution, load cell type, flat indenter type, cartilage layer thickness and stress-relaxation parameters.

# CONFINED COMPRESSION OF A CARTILAGE DISK

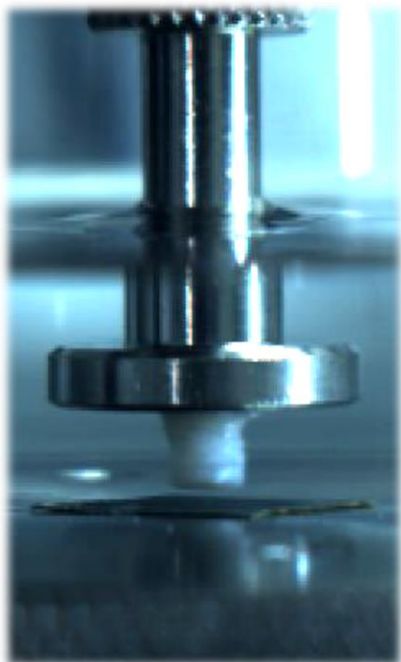


## Purpose

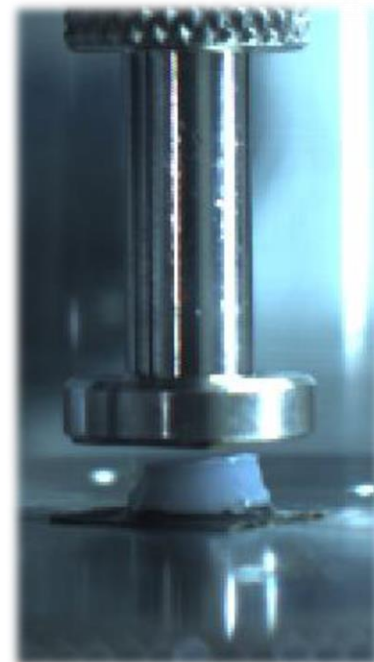
This procedure describes a standard method to realize confined compression of a cartilage disk using the Mach-1™ mechanical tester. Analysis of the measurement results is part of a companion document (SW186-SOP05-D)

## Scope

Under confined compression configuration, stress-relaxation protocol is often used. Using a displacement-control approach, strain ramp(s) followed by relaxation plateau(s) is generally applied at constant strain rate while the sample reaction force is measured. Confined compression is characterised by a uniaxial deformation and a multiaxial loading. Fluid flow is forced out from the cartilage in the vertical direction only using impermeable confinement walls and porous compression platen(s). At equilibrium, the exudation of the fluid ceases. The aggregate modulus ( $H_A$ ), the hydraulic permeability ( $k$ ) and the relaxation time ( $T$ ) can be extracted from a confined compression test.



## SHEAR TESTING ON A CARTILAGE DISK OR AN OSTEOCHON DRAL CORE



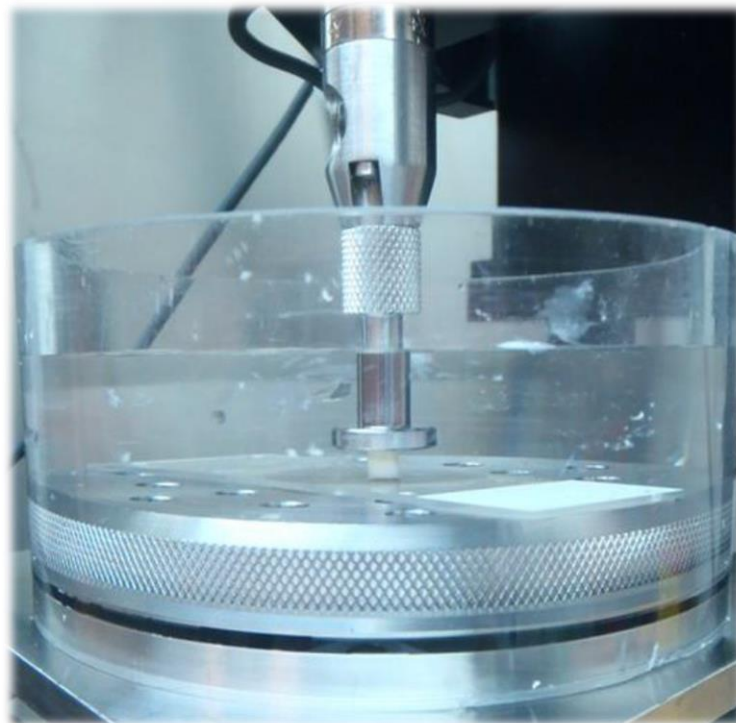
### Purpose

This procedure describes a standard method to realize a planar or a torsion shear test on an articular cartilage disk or an osteochondral core using the Mach-1™ mechanical tester. Analysis of the measurement results is part of a companion document (SW186-SOP06-D)

### Scope

This procedure can be used for the *ex vivo* planar or torsion test on an articular cartilage disk or an osteochondral core. It is highly recommended to use a standard protocol for sample preparation to allow a better control on sample' s dimensions and to facilitate positioning in the chamber. Some parameters must be specified in an associated protocol/report: planar or torsion shear, sample type, thickness of the cartilage layer of each osteochondral core, sample diameter, vertical resolution, sample' s attachment methods, flat indenter type, filename, stress-relaxation parameters and number of ramps.

# FRICTION TESTING ON A CARTILAGE DISK OR AN OSTEOCHONDRAL CORE



## Purpose

This procedure describes a standard method to realize a friction test on an articular cartilage disk or an osteochondral core using the Mach-1™ mechanical tester. Analysis of the measurement results is part of a companion document (SW186-SOP07-D)

## Scope

This procedure can be used for the *ex vivo* friction test using a planar sliding method on an articular cartilage disk or an osteochondral core. It is highly recommended to use a standard protocol for sample preparation to allow a better control on sample's dimensions and to facilitate positioning in the chamber. Some parameters must be specified in an associated protocol: filename, cartilage thickness relaxation parameters, move relative parameters, ramp release parameters, lubricant (optional) and sliding counter surface.



## EXTRACTION AND PREPARATION OF CARTILAGE DISKS AND OSTEOCHONDRAL CORES FROM AN ARTICULAR SURFACE

### Purpose

This procedure describes a standard method to extract and prepare cartilage disks and osteochondral cores from an articular surface.

### Scope

This procedure can be used for the *ex vivo* collection of disks or cores from an articular surface of large species (rabbit size to larger species such as horse). Some extraction parameters must be specified in an associated protocol: diameter of the osteochondral cores or disk extracted.

# EXTRACTION OF ARTICULAR SURFACES FROM A CLOSED STIFLE JOINT IN LARGE ANIMAL SPECIES



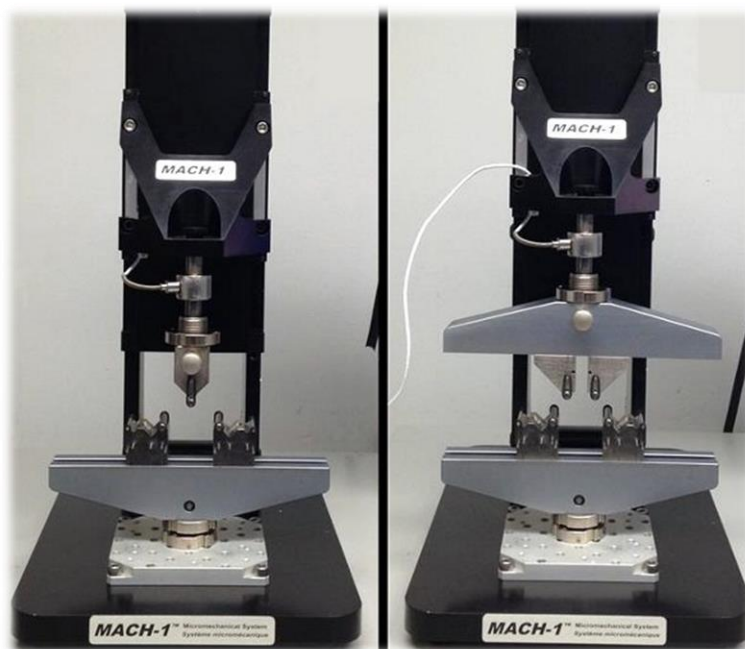
## Purpose

This procedure describes a standard method to extract articular surface from a closed stifle joint in large animals.

## Scope

This procedure can be used for the stifle joints of large animals. Following this protocol will ensure that samples tested will have the same uniform surface positioning/orientation. It is also highly recommended to use our guidance for preservation of the articular surface extracted.

# 3-POINT OR 4- POINT BENDING



## Purpose

This procedure describes a standard method to realize a flexural (3-point and 4-point) bend test on a material sample using the Mach-1™ mechanical tester. Analysis of the measurement results is part of a companion document (SW186-SOP08-D)

## Scope

This procedure can be applied on any type of material with shape and dimension compatible with the specifications presented in the material section while the expected experimental displacements, strain rates, forces or torques remain within tester specifications. Some parameters must be specified in an associated protocol/report: 3 or 4-point setup selection, loading pin sizes, sample geometry, vertical stage resolution, filename, bending test parameters.

# Lap Shear Testing



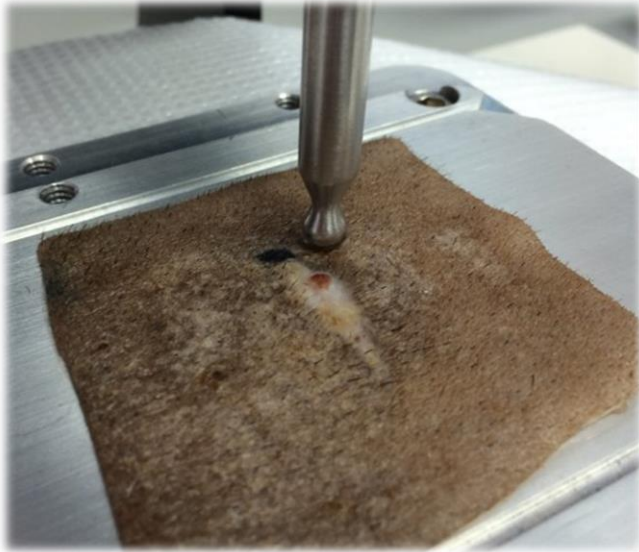
## Purpose

This procedure describes a standard method to realize a lap shear test on an adhesive between two substrates using the Mach-1™ mechanical tester.

## Scope

This procedure can be used for a lap shear adhesion testing. Some parameters must be specified in an associated protocol/report: thickness of the substrate, composition of the adhesive (molecular weight, molecular composition, final geometry), vertical resolution, substrate attachment method, filename, stress-relaxation parameters and number of ramps. Note that for the case of gel adhesive, instructions for the preparation of the gel layer using a kit (MA133) are also included. It is highly recommended to use a standard protocol for sample preparation to allow a better control on sample's dimensions and to facilitate positioning in the chamber.

# Case Studies



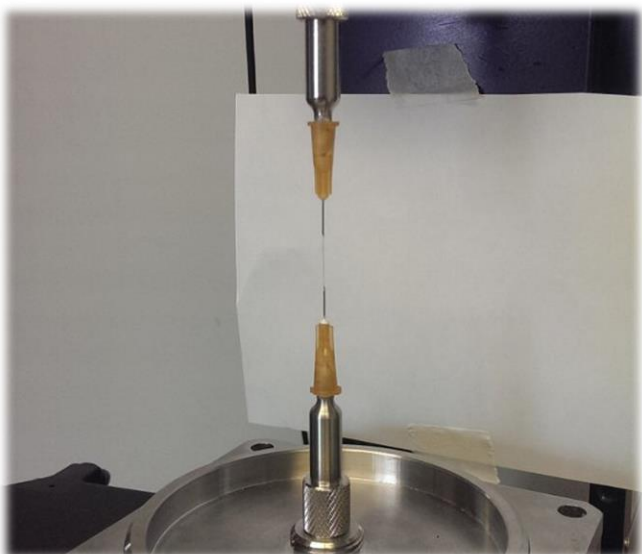
## INDENTATION MAPPING ON 36 PIG SKINS FOR A FULL THICKNESS

A world-wide renowned Pharma needed to mechanically characterize the healing of skin in a model of full thickness excision. To address their needs, we designed a non-GLP study to perform the mechanical characterization of the samples the client sent to us. This characterization used two test configurations, namely indentation mapping and tensile testing.

Indentation mapping is a non-destructive technique in which automated indentation is performed throughout the surface of the sample. This technique has several advantages: it is non-destructive and allows the same sample to be used for other tests (e.g. tensile testing in this case) or characterization (e.g. histology). From the recording of each indentation, several mechanical properties can be obtained including the thickness, the structural stiffness and the instantaneous shear modulus. Combined with the positional information of each recording, the topography of the skin can be obtained and distinctive maps for each mechanical properties can be calculated. For this pilot study, maps for the thickness, structural stiffness and the instantaneous shear modulus were generated. From these maps, the area of the “wound” or the “affected skin” were assessed.

Due to the non-invasive nature of the indentation, the second approach used in this study was to perform tensile testing on the same sample to determine the load at rupture.

Following the completion of this pilot study, several other studies were conducted for this client using these characterization techniques.



# EVALUATION OF THE MECHANICAL PROPERTIES

We were recently asked if our mechanical tester has the capability of evaluating the mechanical properties of single fiber human hair. In our lab, a scientist has been devoted to this feasibility study.

The hardest part of this work was to develop the proper gripping fixtures to easily mount the hair on the tester to be able to perform tensile and torsion testing. Following few attempts, it was found that the simplest and most reproducible mounting method was based on the use of a pair of off-the-shelf syringe needle tips. On the bench, the hair fiber was inserted through the two needles facing each other and spaced by a predefined gauge gap. A single drop of cyanoacrylate glue was applied in the plastic cavity of each needle to secure the hair in place. Two needle tip holders with the same tapered shape as a regular syringe were mounted on the Mach-1™. These two holders were fastened facing each other at the center of a testing chamber under a 17N multi-axis load cell. The double-needle hair assembly was then firmly inserted over the holder.

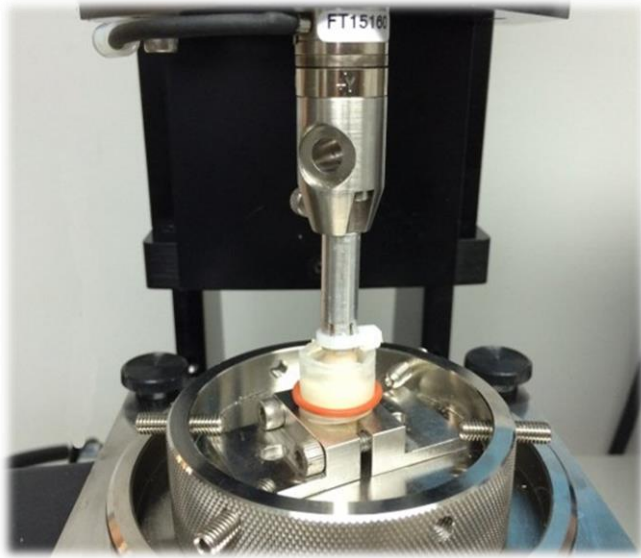
After zeroing the load, and considering the relative position of the vertical stage, the initial length of the hair at full extension (when no load is applied) was measured using the Mach-1 Motion's "Find Contact" function. A sinusoidal deformation in the elastic region was applied for 30 cycles at 0.5, 1 and 2 Hz. A Dynamic Mechanical Testing analysis was conducted as per MA056-SOP04-D to extract the complex tensile storage and loss modulus components. Dynamic testing showed an increase in phase magnitude with increased frequency. This result was expected and explains an increase in plastic deformation (loss modulus) with increased frequency.

The tensile modulus and ultimate tensile strength were also measured and calculated (Mach-1 Analysis software) during a tensile load ramp to failure - Tensile test output until failure). The results were found to be in accordance with literature (Lee, 2012): 930 MPa ultimate tensile strength, 6.5 GPa elastic modulus. Other tests were completed using a rotational stage to apply torsion to the hair until rupture occurred. For two samples, the results were 175 and 179 turns before failure. A camera feed with a 10X lens was used to visualize the torsion of the fiber in real time.

The plastic torsion of the hair remains even after breakage and can be visualized under a microscope (Post-torsion photograph using 20x microscope).

During torsion, the generated torque around the Z-axis was too low to be measured by the 17N multiaxial load cell. However, the vertical contraction of the hair induced by torsion created a vertical contractile force that was measured by the  $F_z$  channel of the cell. It is assumed that through proper theoretical modelling of this test configuration, this axial load could be used to indirectly measure the torsional shear strength of the hair.

Different indirect ways of quantifying the torsional properties of fibres have also been proposed in literature. For example, by relating the initial gauge length to the number of rotations before rupture, a theoretical value for fracture angle can be obtained. From a basic analysis, the fracture angle was found to be between 26 and 33°.



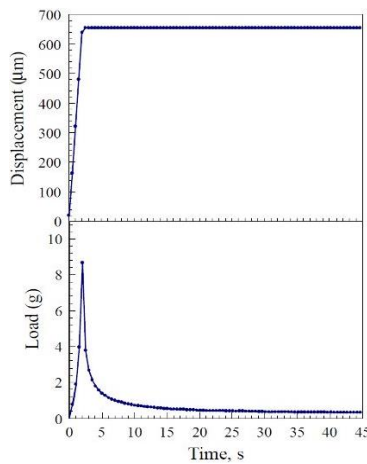
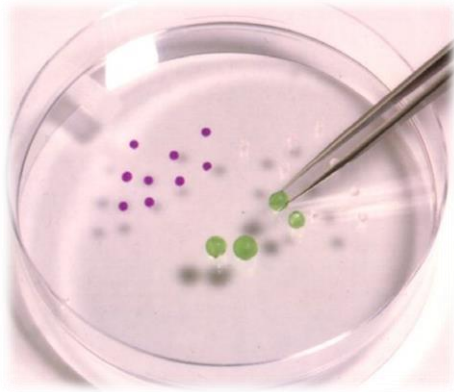
## MEASURING THE COEFFICIENT OF FRICTION BETWEEN TWO CARTILAGE SURFACES IN ROTATION

Our articulations have evolved to permit a near frictionless movement of the joint; the coefficient of friction of cartilage is so low that it can be very difficult to measure. One of our clients has developed an innovative test protocol to measure both the static and the dynamic friction coefficients. This client was also interested in knowing the effect of the waiting time, before initiating the movement, on the static friction coefficient as well as the effect of the lubricant (PBS or synovial fluid) on both coefficients.

We have worked with him to adapt his test protocol and experimental setup to our Mach-1 v500ct multiaxial mechanical tester. From the flat portion of the trochlear groove of bovine femoral heads, large cylindrical osteochondral cores (2 different diameters) were harvested. The core with the large diameter was carefully press-fit into a clear flexible tubing (to create a wall to contain the lubricant) and fixed on a secured holder attached to the rotational stage of the Mach-1. The smaller diameter piece was attached under the multiaxial load cell using a custom attachment fixture.

After filling the chamber with lubricant (either PBS, a negative control, or synovial fluid), the upper cartilage surface was placed in contact with the opposing cartilage surface with a vertical offset load applied. Using the rotational stage, both surfaces were rotated against each other after predefined waiting periods. After some adjustments were made to consider the geometry of the test configuration, the coefficients of friction were calculated using the torque value along the vertical axis ( $T_z$ ) divided by the vertical force ( $F_z$ ) measured between the surfaces. The static coefficients of friction were calculated based on the required torque to initiate the movement after a certain resting period, while the dynamic coefficients were calculated using the torque measured when a specific rotation speed was reached.

The results obtained were in line with the literature for the magnitude of the coefficient of friction and, as expected, confirms the positive impact of the synovial fluid in the reduction of the coefficients of friction in the articular joint.



*Relaxation curve*

## CHARACTERIZATION OF THE MECHANICAL PROPERTIES OF ALGINATE BEADS

Alginate beads are used extensively in the biomedical industry. Mechanical properties of alginate beads with diameters smaller than 1 mm can be precisely measured with the Mach-1.

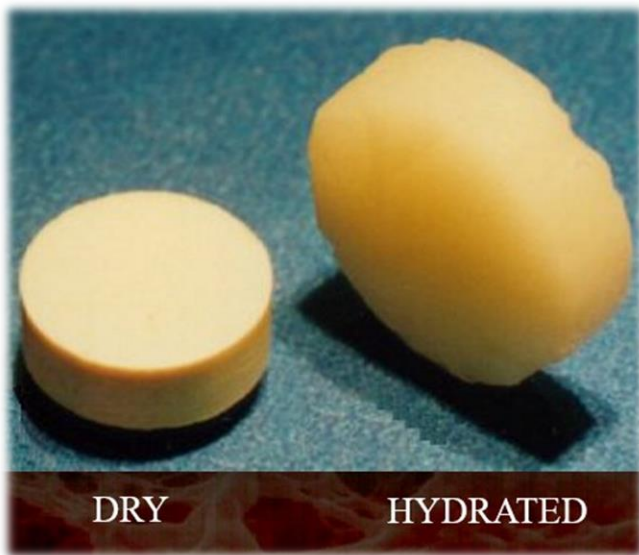
Two types of beads with different  $\alpha$ -L guluronic content or G-content

(LVM with 13% and LVG with 70%) were tested under unconfined compression in 0.15 M NaCl and in 50 mM CaCl<sub>2</sub> solutions following a 30 minutes equilibration. A compression ramp of 50% of the bead diameter was applied in 2 seconds and an equilibrium endpoint was assumed to be a load relaxation rate of 0.05 g/min.

The Mach-1 is designed for various testing protocols including stress relaxation, dynamic sinusoids and creep. A typical result of a stress relaxation test with an LVG sample in CaCl<sub>2</sub> solution can be seen. Table 1 summarizes the mechanical properties of the two types of beads in the two testing solutions (refer to related resource file).  $N$  is the number of samples,  $D$  represents the sample diameter,  $F_t$  is the transient load,  $F_{eq}$  is the equilibrium load,  $t_1$  is the time when half the peak load is obtained during the ramp and  $t_2$  is the time when half of the transient load is relaxed.

We have observed that LVG beads with 70% G-content were larger than LVM beads with 13% G-content. LVG beads were also stiffer than LVM beads in the two solutions. However, LVM beads seemed to have a weakening reaction with calcium. In fact, LVM beads are stiffer and relax more slowly in 0.15 M NaCl than in 50 mM CaCl<sub>2</sub>. High G-content increases bead stiffness and appears to diminish sensitivity to the presence or absence of calcium.

The high accuracy of the mechanical tester was needed to obtain precise data on bead mechanical properties with diameters smaller than 1 mm. The Mach-1 is a flexible system adapted for highly sensitive and precise testing of many types of samples (biomaterials, microspheres, pills, living tissues, etc.) in controlled environments (incubators). Its ease of use and modular software offers unlimited testing



## CHARACTERIZATION OF THE MECHANICAL PROPERTIES OF PHARMACEUTICAL TABLETS

In this study we investigated the swelling behavior and mechanical properties of pharmaceutical tablets used for controlled drug release. Such information can guide understanding of the influence of swelling, hydration, and structural rigidity on release kinetics.

The tablets were tested in a chamber filled with distilled water after  $71 \pm 3$  hours of hydration and swelling in distilled water. The mean thickness ( $5.44 \pm 0.97$  mm) and diameter ( $5.76 \pm 0.01$  mm) mm of the tablets were measured with a micrometer. Stress relaxation measurements were performed on four types of samples characterized by different compression forces on the powder during the fabrication and dry hardness (See Table 1). During mechanical testing, a first compression step at low velocity is applied to compress the tablet to a uniform thickness. Then, 4 small compression steps of 1% of the thickness are applied at a velocity of 0.2%/s with a relaxation time of 10,000 seconds after each step. This is followed by 4 steps of release using the same conditions.

Table 1: Physical Characteristics of Fabrication

Sample	Compressive force	Sample
1	4.17	141
2	6.3	175
3	10.6	198
4	13.6	206

A typical stress relaxation test curve for Sample 2 is shown. These results show that swollen tablets successfully withstand the imposed loading protocol since they have a nearly reversible behavior with similar equilibrium loads during compression and release. The peak load, however, is higher during

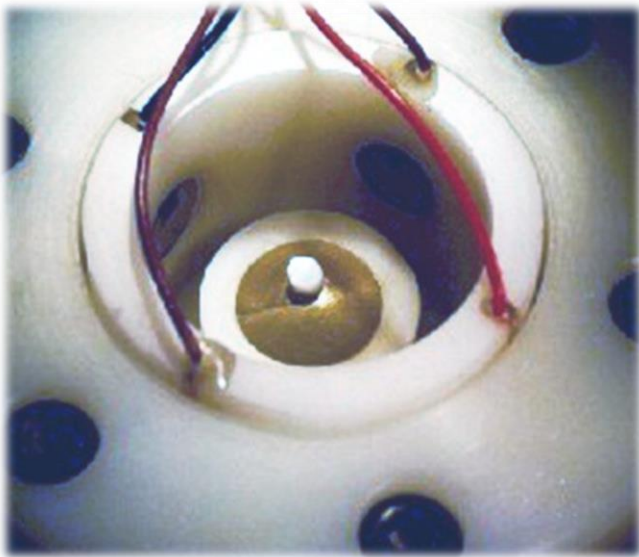
compression compared to release. The equilibrium stiffness of the tablets is also shown to increase with compression. Interestingly, the equilibrium stiffness decreases with compression force applied to the powder during fabrication and with the dry hardness of the tablet.

A creep test was used in this study to observe swelling and the evolution of mechanical properties during swelling. Swelling of Sample 2 in distilled water for 5 hours is shown. A compression ramp of 20 mm at a velocity of 4 mm/s with a relaxation time of 10 s was applied every half hour during swelling. The tablets swelled by 700  $\mu\text{m}$  during 5 hours. Furthermore, the mechanical properties are quite different for dry tablets ( $t=0\text{s}$ ) compared to the hydrated tablets. Swelling of the tablet alters its structure so that the dynamic stiffness is reduced by a factor of 3 after 5 hours of hydration and swelling.

Data from mechanical tests can be analyzed to obtain structural information. Using a fibril-network reinforced poroelastic model developed for tissue mechanics, the stress relaxation curves can be processed to obtain four model parameters: matrix equilibrium stiffness ( $E_m$ ), hydraulic permeability ( $k$ ), matrix Poisson's ratio ( $\nu$ ) and fibril network stiffness ( $E_f$ ) (refer to Soulhat et al 1999 on this website).

$k$  can be directly related to pore size and thus drug transport of the tablets.  $E_m$  can be related to the stiffness of the central part of the tablet and  $E_f$  to the stiffness of the membrane surface layer. In fact, during swelling, we observed that tablets are characterized by a surface layer with properties different from the central portion. Results were obtained by fitting the stress relaxation curves with the model. Interestingly,  $E_f$  is higher and  $k$  is smaller in compression than in release.  $E_f$  is directly related to the peak load which is lower in release. The increase of  $k$  can be explained by the fact that the tablet continues to swell during compression. Microstructural information can be further obtained by using the Navier-Stokes equations to estimate the pore size of the matrix. The resulting pore size of the matrix varies between 5 and 15 nm, increasing during hydration.

In this case study, we have shown that the Mach-1 can precisely measure the mechanical properties of swollen pharmaceutical tablets. Critically important information was obtained showing that the mechanical properties of dry tablets (compression force of the powder and hardness) differed drastically from those of hydrated tablets. Furthermore, we hypothesize that the mechanical behavior of hydrated tablets are more closely related to events controlling the drug release. In fact, we observed that after 71 hours of swelling, the equilibrium stiffness is higher for tablets manufactured with a smaller force of compression on the powder. This may be explained by the presence of defects or cracks in harder tablets manufactured with higher compression forces. Results not shown also indicated that mechanical properties of hydrated tablets are influenced by the salt concentration and pH of the test solution.



## CHARACTERIZATION OF ELECTROMECHANICAL PROPERTIES OF CONNECTIVE TISSUES - PART 1 - ARTICULAR CARTILAGE

In this case study, the Mach-1 mechanical tester was used to determine the electromechanical properties of two connective tissues: the cartilage and the meniscus. Since tissue stiffness and compression-generated electric fields, or streaming potentials, are sensitive to the biochemical content of the tissue, the tester was coupled with an array of electrodes that can precisely measure these electric signals. The objective of this study was to establish links between biochemical composition and electromechanical properties (stiffness and streaming potentials) of normal and degenerated connective tissues. The first part of the study focuses on articular cartilage.

Since the articular cartilage extracellular matrix is primarily composed of negatively charged proteoglycans entrapped in a collagen network, there is an excess of mobile positive charges in the fluid. Compression of the cartilage produces streaming potentials via the separation of positively charged mobile ions relative to the fixed negatively charged proteoglycans.

Matched pairs of bovine cartilage/bone disks (3 mm in diameter) were cultured with and without a degradation agent (interleukin-1 or IL-1) for 11 days.

Electromechanical properties of the cartilage were evaluated by incorporating an array of electrodes into a testing chamber mounted on the Mach-1. The Mach-1 is designed for various testing protocols including stress relaxation, sinusoidal displacement and creep in different configurations (confined and unconfined compressions, tension, indentation and bending). In this study, streaming potentials across the tissue surface are measured in unconfined compression geometry with a linear array of 8 platinum electrodes of 50  $\mu\text{m}$  diameter separated by 300  $\mu\text{m}$ . Electrodes 1 to 6 covered the 1.5 mm cartilage disk radius, and electrodes 7 and 8 were external to the cartilage in the bath. The testing chamber was filled

with physiological saline solution. A static compression offset of 100  $\mu\text{m}$  was applied in a sequence of small step compressions of 20  $\mu\text{m}$  at 2  $\mu\text{m/s}$ . Dynamic sinusoidal tests were performed at frequencies of 1, 0.1 and 0.01 Hz with displacement amplitudes of 8, 4 and 2  $\mu\text{m}$ . The streaming potential radial profile was constructed by the addition of each channel in the complex domain. Proteoglycan or glycosaminoglycan (GAG) content in the disk and content lost to the media during the culture was measured with the dimethylmethylene blue dye and spectrophotometry.

Figure 3 shows the GAG content in cartilage disks during the culture. The IL-1 treated disks lost 10, 20, 65 and 75% of their GAG content after 1, 4, 7 and 11 days of culture respectively. The Mach-1 is easy to use and its modular software permits a direct and rapid analysis of the dynamic sinusoidal test results. Figure 4 shows that dynamic stiffness was 3 times lower for the IL-1 treated disks compared to control after 11 days of culture.

The analysis of the stress relaxation test results showed that, at the end of the culture, the static stiffness was 4 times lower for degraded disks compared to control (0.3 MPa). Figure 5 shows the streaming potential profiles after 11 days of culture for normal and degraded cartilage. We observed that the profile potential gradient at the periphery for the IL-1 treated explants was reduced by half compared to control disks only one day after the beginning of the culture. The potential profile amplitude at the center of the disk was significantly lower for degraded disks compared to control explants after 7 days of culture.

The Mach-1 mechanical tester coupled with an array of electrodes can precisely determine the electromechanical properties of a large range of normal and degraded connective tissues.

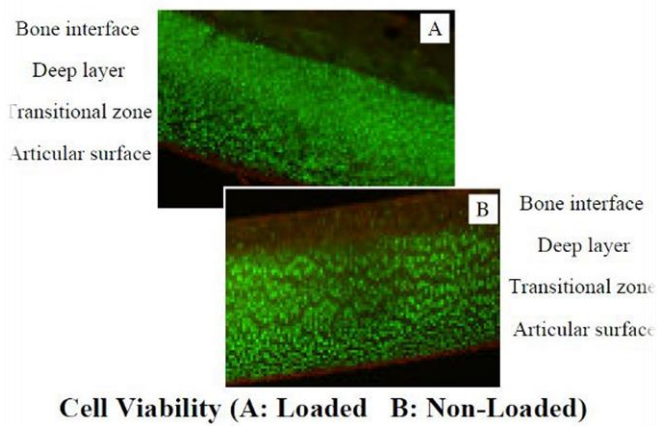


## CHARACTERIZATION OF ELECTROMECHANICAL PROPERTIES OF CONNECTIVE TISSUES - PART 2 - MENISCUS

In this case study, the Mach-1 mechanical tester was used to determine the electromechanical properties of two connective tissues; the cartilage and the meniscus. Since tissue stiffness and compression-generated electric fields, or streaming potentials, are sensitive to the biochemical content of the tissue, the tester was coupled with an array of electrodes that can precisely measure these electric signals. The objective of this study was to establish links between biochemical composition and electromechanical properties (stiffness and streaming potentials) of normal and degenerated connective tissues. The second part of the study focuses on meniscus.

The meniscus is a tissue similar to cartilage but softer and less charged. In this case, the samples have been sectioned to five 3-mm disks (about 1-2 mm thick) from various specified regions. Dynamic stiffness under unconfined compression and the streaming potential distribution are measured. It should be noted that the streaming potential are around 10 times lower for meniscus than cartilage (refer to Part 1 of this case study). These results also indicate that the dynamic stiffness and the streaming potential profiles are higher on the cartilaginous surface of the inner part of the meniscus (disk 1 and 2) compared to middle zones (disks 3 and 5). It is expected that these results are directly related to the proteoglycan content of menisci.

The Mach-1 mechanical tester coupled with an array of electrodes can precisely determine the electromechanical properties of a large range of normal and degraded connective tissues.



# IN VITRO MECHANICAL STIMULATION OF ARTICULAR CARTILAGE

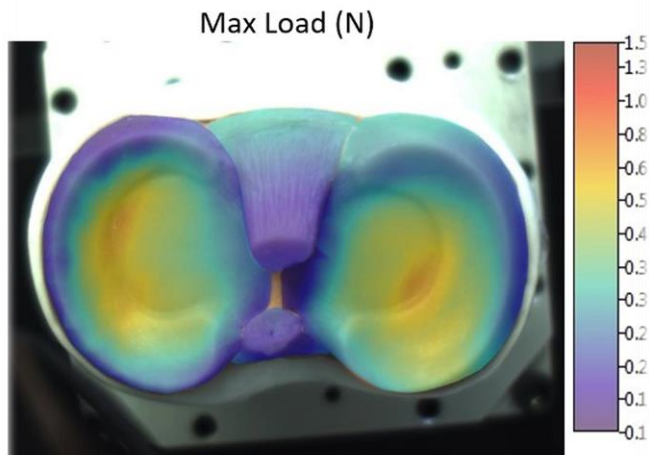
The Mach-1 can be used as an in vitro mechanical stimulation device inside an incubator and in a sterile controlled environment. Mechanical stimuli can modulate anabolic or catabolic processes in cell or tissue cultures. The flexible user friendly software available on the tester and the displacement and force resolutions of 100 nm and 0.1 mN are unique to this system and of great practical importance in tissue engineering studies. The versatile nature of the tester components and its sophisticated and flexible software allowed us, in this study, to: 1) stimulate tissue matrix synthesis and assembly and 2) provoke structural damage followed by either repair processes or progressive degradation, the latter being a sign of osteoarthritis. Our hypothesis: high amplitude mechanical load can be damaging to cartilage extracellular matrix as reflected by increased collagen denature in loaded tissue explants. Physiological dynamic loading can modulate type II collagen synthesis reflected by the content of its c-propeptide CPII.

In vitro loading was performed 2 days following disk isolation in uniaxial unconfined compression. Pairs of disks were transferred to a sterile dynamic compression chamber containing culture media, and subsequently mounted onto the tester in the incubator. Disks were subjected to different loading protocols depending on the desired effects: degradation or stimulation. The degradation loading protocol was 40 cycles of 250  $\mu\text{m}$  in amplitude with a speed of 100  $\mu\text{m}/\text{s}$  while the stimulation protocol was 10 ramp/release of 100  $\mu\text{m}$  amplitude during one hour per day for five consecutive days.

The high amplitude loading protocol with the Mach-1 inside a tissue incubator did not alter cell viability of the intact full-thickness cartilage/bone explants (green=live cells, red=dead cells). Peak stresses were shown to be between 2 to 4 MPa using the high amplitude loading protocol. 40 cycles of this compressive load induced an enhancement of degraded collagen in the loaded samples. A smaller compression

amplitude for a longer duration was shown to stimulate collagen synthesis, demonstrating the potential need for mechanical stimuli to produce tissues in vitro.

The Mach-1 can be used to precisely apply mechanical stimulation to living tissues in standard tissue culture incubators. It is particularly well suited for tissue engineering applications where loading protocols can be refined to produced desired effects on tissue metabolism and growth.

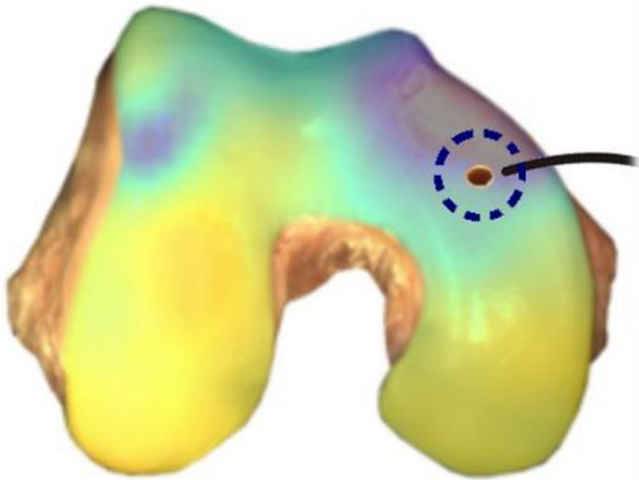


# CHARACTERIZATION OF A SAWBONES TIBIAL

For the demonstration of the 3D mapping capabilities of our Mach-1 model v500css mechanical tester at our exhibition booth at trade shows and scientific conferences, we use a human tibial plateau replica from Sawbones. Obviously, this is much more convenient than carrying a real human sample in our luggage! While the bone is made of plastic, the articular surface (in fact, the meniscus merged with the cartilage surface and the cruciate ligaments) is molded in a rubber-like material. Here, we summarized the method used to obtain the 3D surface profile, the rubber thickness and stiffness maps.

The tibial plateau replica was mounted on the mechanical tester platform and a top-view picture was taken using the Mach-1 camera. With the Mapping Toolbox software, a position grid (about 300 positions) was superimposed over the picture and two reference positions were used to convert the pixel coordinates of each position into real XY tester coordinates. Using the "Normal Indentation" function of the Mach-1 Motion software, the surface was scanned using a 2-mm diameter spherical indenter. At each location, the indenter is gently lowered toward the surface until a light contact (10 g) is detected by the load cell which indicates the surface height (or thickness) and orientation. Then, a 500-micron indentation (normal to the surface) is made by moving the three stages at different speeds and by measuring the normal component of the load (using the multi-axis load cell). The maximum load at each point is then plotted over the initial photo to obtain a mapping. Using the theoretical Hayes elastic model in spherical indentation, the normal indentation curve can be fitted (with the local thickness) to obtain the apparent local stiffness of the material (also mapped).

Since the articular surface is molded in a single homogeneous rubber-like material, one could expect a more uniform stiffness mapping. Even if the topographical variations observed in the maximum force mapping can, in principle, be explained by the thickness variation through the Hayes model, some minor variations remains in the stiffness map. This is explained by the fact that the Hayes model assumed a flat slab of material. To remove all variations, a finite-element model would be a more robust approach. At the center of the tibial plateau (a relatively flat region) material stiffness was about 1 MPa while the stiffness of normal human articular cartilage at this location is around 2 MPa (so not very far from what would be felt by a surgeon probing). However, real cartilage exhibits a more complex poroelastic behavior, while the replica is purely elastic.



## SEQUENCE OF MECHANICAL TESTS FOR ARTICULAR CARTILAGE AT A SINGLE LOCATION

In a recent study, our group has highlighted the importance of considering the natural topographic variability of the mechanical properties of cartilage over the articular surface, particularly in the context of cartilage repair, where one can assess the effect of treatments. Moreover, the availability of test samples is limited in repair studies since the regions of interest are of limited size. A solution to overcome this problematic is to perform multiple tests at a single location over the articular surface. Therefore, the objective of this study was to develop a sequence of mechanical tests to characterize articular cartilage at a single location.

Significance: The use of a sequence of tests can minimize the number of required samples and minimize the impact of the natural variation of the mechanical properties in data analysis.

### Tissue Source

6 osteochondral cores (D= 3.5 mm), Extracted from 5 distal femurs, Healthy cadaveric human joints, provided by RTI Surgical (Florida).

### Sequence of tests

Note: 10 minutes wait was allowed between each test and tests were performed in PBS

#### Step 1: Automated Indentation and Thickness Mapping

Automated Indentation Technique allowed measuring mechanical properties over the entire surface

The thickness is obtained with an adapted version of the needle technique

Instantaneous modulus (IM) extracted by an elastic indentation model

IM and cartilage thickness (h) of each core was calculated as the average of all values measured within 6 mm from the core center

## Step 2: Thickness under dissection microscope

Cartilage thickness ( $h$ ) was re-measured using a dissection microscope

## Step 3: Friction

20% equilibrium strain was applied.

Friction test was executed following a 5 mm circular path (1440° rotation) on glass.

Coefficient of friction at equilibrium  $\mu_{eq}$  was extracted.

## Step 4: Unconfined compression

10% precompression

Followed by 5 ramps of 2% stress relaxation

Data were fit to a poroelastic model with fibril reinforcement to extract the matrix modulus ( $E_m$ ), fibril modulus ( $E_f$ ) and radial permeability ( $k_r$ )

## Step 5: Shear

Sandpaper (1500 grit)

Shear modulus ( $G$ ) at 10%, 15% and 20% compression was extracted

## Step 6: Confined Compression

10% pre-compression

Followed by 5 ramps of 2% stress relaxation

Data were fit to a linear biphasic model where the aggregate modulus ( $H_A$ ) and axial permeability ( $k_z$ ) were extracted

## Results

The results present the extracted parameters of the 6 cores from the various test configurations (at 20% strain).

A significant correlation ( $r=0.81$ ,  $p=0.05$ ) was observed between the thickness obtained with the automated thickness mapping (Step 1) and the thickness obtained under the dissection microscope (Step 2)

The coefficient of friction values are generally higher than stated in the literature, but the reference values found for cartilage on glass in PBS were done on bovine cartilage, which might not be comparable.

$E_m$  is approximately 15 times lower than  $E_f$ , which is expected and reported in the literature.

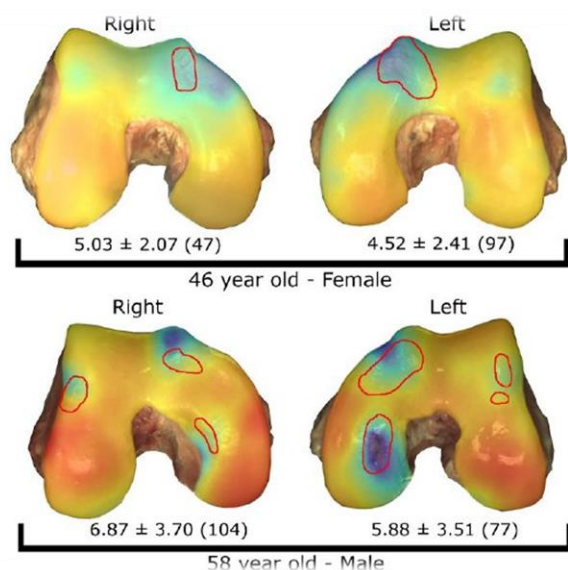
$G$  are in the same range than those reported in the literature.

$H_A$  and  $k_z$  from confined compression tests are similar to those reported in the literature.

The hydraulic permeability in the axial (confined compression) and radial (unconfined compression) direction have a 10-fold difference for a compression higher than 10% as stated in the literature.

### Discussion

The variability between the individual 6 samples in these measurements arises from the spatial distribution pattern since samples are not taken from the same compartment on the articular surface. The sequence of mechanical tests for articular cartilage at a single location appears to be promising since it provides values consistent with those reported in the literature. Additional analyses such as histological or biochemical assessments can be performed after this sequence of mechanical tests on the same sample. For future studies, it will be interesting to test cartilage at different states of degeneration to determine which mechanical parameters are more sensitive to degradation and to investigate a correlation between these parameters and additional analyses.



## IDENTIFICATION OF EARLY DEGENERATED (OSTEOARTHRITIS-LIKE) REGIONS OVER ENTIRE ARTICULAR

A currently unsatisfied need in arthritis and cartilage research is the *ex vivo* functional assessment of an entire articular cartilage surface both quantitatively and non-destructively. The objective of this study was to investigate the ability of a novel automated technique to characterize the mechanical properties of entire articular surfaces in indentation in order to rapidly discriminate between degenerated versus healthy articular cartilage.

Method

Sample

Complete articular surfaces from 8 human distal femurs were obtained from RTI Surgical, FL. Articular surfaces were attached to a testing chamber filled with PBS and equipped with a camera-registration system (1 mm registration resolution). A position grid was superimposed on the image of the sample. Articular surfaces were visually graded using the ICRS system:

ICRS 0 (visually normal, outside circled regions in Images 4 & 5)

ICRS > 0 (visually abnormal, inside circled regions in Images 4 & 5)

Automated Indentation Mapping

A spherical indenter (radius = 3 mm) for this new automated indentation technique.

A multiaxial load cell uses  $F_x$ ,  $F_y$  and  $F_z$  to calculate the normal force.

A 3-axis mechanical tester (Mach-1 v500css) uses 3 displacement components simultaneously to perform a perpendicular displacement based on the measured surface orientation.

Steps performed at each position:

- 1) Measure the contact coordinates at a predefined position
- 2) Measure the contact coordinates of 4 surrounding positions
- 3) Calculate surface orientation using the contact coordinates
- 4) Perform perpendicular indentations and measure the normal force

### Automated Thickness Mapping

A needle probe replaces the spherical indenter.

A load cell uses  $F_z$  to calculate the force.

Thickness measurements use a needle penetration technique.

Mapping of cartilage vertical distance over the entire articular surface.

Cartilage thickness was calculated using the surface orientation previously obtained.

Thickness = Vertical distance x cosine (surface orientation)

### Instantaneous Modulus Calculation

The instantaneous modulus at each position was obtained by fitting the load-displacement curve (with corresponding thickness) to an elastic model in indentation.

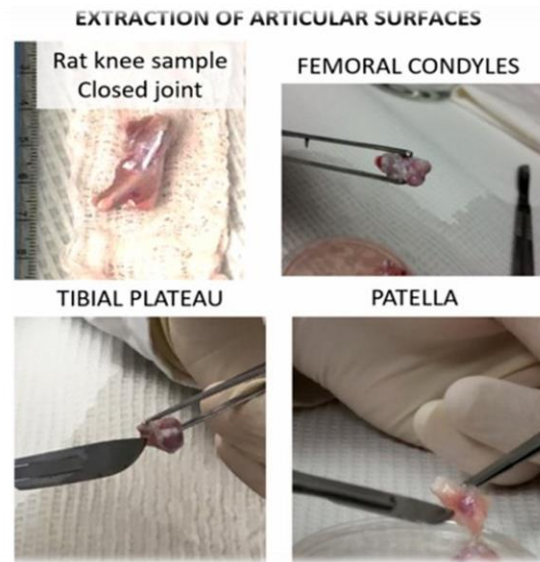
Results

The mappings reveal patterns of thickness and instantaneous modulus that are spatially correlated and symmetric for right and left joints of the same donor. Using a one-way analysis of variance (ANOVA), a significant difference in thickness and instantaneous modulus distributions was found between the donors ( $p < 0.0001$  for both) while there was no significant difference within each pair of donors ( $p > 0.1$  for both). Values obtained for thickness are in agreement with previously reported data for human femoral cartilage.

Thickness mappings are more uniform than the instantaneous modulus mappings and the thickness patterns do not correlate with the visual assessment of abnormal cartilage (ICRS > 0). Instantaneous modulus, measured in indentation over the entire surface, identifies and quantifies the visually identified abnormal regions and shows degradation patterns that often extend the visual lesion boundaries. These regions show much lower instantaneous modulus (between 0.2 and 3 MPa, blue-green regions in than the average instantaneous modulus measured. Excluding sample preparation time, the acquisition of each pair of thickness and indentation mappings takes 1 minute/position of machine time and 30 minutes/pair of joints of data post-processing.

### Conclusion

In contrast to what is usually required for traditional biomechanical testing (i.e. individual sample harvesting, visual orientation of the sample surface perpendicularly to compression axis, sample preservation causing possible mechanical alteration), this technique does not require interventions that are costly and time-consuming, thus considerably reducing sources of measurement error and allowing for high resolution mappings of the entire articular surface. The results of this study clearly demonstrate the capabilities of this novel automated indentation technique to rapidly, objectively and non-destructively map the biomechanical properties of full articular surfaces and to identify degenerated regions. This automated indentation mapping technique will be of great value in the identification of wear patterns in OA progression and in cartilage repair studies.



## INDENTATION AND THICKNESS MAPPING ON RAT KNEE ARTICULAR SURFACES AFTER MEDIAL

Dr. Evseenko from University of Southern California contacted us to incorporate mechanical testing into one of his studies: "How does medial meniscal tear (MMT) affect the joint in a rat model". A major challenge in characterizing the outcome of this degenerative model is related to the very small size of the samples. To demonstrate the performance and sensitivity of our mechanical mapping technique in detecting potential osteochondral changes a few weeks following surgery, our scientists - in collaboration with Dr. Evseenko's lab - designed a short pilot study.

Following our procedure for the importation of biological samples, 2 closed murine knee joints from the same animal (right contralateral control joint and left joint with the MMT surgery) were shipped overnight to our facility. Upon arrival, our study director, experienced with handling small animal joints, carefully extracted the tibial plateaus, distal femurs and patellas. Each articular surface was then attached onto our multiaxial mechanical tester (Mach-1 model v500css equipped with a 17N multiaxial load cell, a spherical indenter ( $D=0.5$  mm) and a 26G needle probe) to perform automated indentation and thickness mappings. Following these non-destructive tests, samples were fixed, packaged and shipped back for subsequent histological analyses.

Using the normal stress-relaxation curves (normal spherical indentation) and the load vs displacement curves (needle penetration), analyses were performed to calculate instantaneous modulus (MPa) and cartilage thickness (mm) at each position of the mapping. These high-resolution mappings (~80 positions/surface) allowed the detection of stiffer regions (suggesting bone exposure) surrounded by abnormally softer cartilage in the medial side of the tibial plateau and femoral condyles (kissing lesion) of the treated left knee, when compared with the untreated right control knee. Mappings of the tested

patellas also revealed a drastic decrease of cartilage stiffness of the treated knee compared to the control. These pilot results demonstrated the potential of this technique in understanding the functional impairment in knee joints following MMT surgery and in following the evolution of the induced degeneration.

This pilot study (from the sample reception to preliminary report submission) was completed within 2 days. Dr. Esveenko has given his consent to publish this case study.

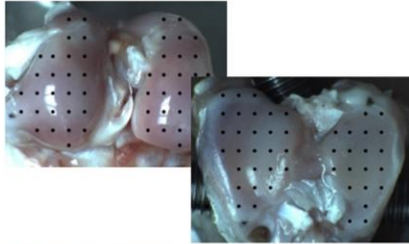
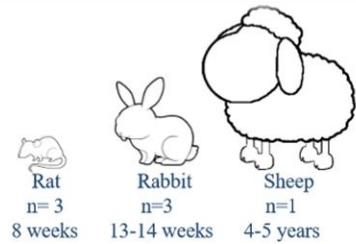


**Fig.1:** Top view image of the articular surfaces (rabbit presented) with position grid superimposed.

## RELEVANCE OF THE SPATIAL DISTRIBUTION OF MECHANICAL PROPERTIES OF ARTICULAR

In order to evaluate the effect of cartilage treatments, appropriate control sites need to be chosen. However, finding the right location for the control site is quite challenging in articular surfaces where a natural spatial distribution of mechanical properties is present in all healthy joints. The purpose of this study was to assess the importance of considering the spatial distribution of the mechanical properties of normal articular cartilage in animal models of cartilage repair, specifically the distributions of thickness and instantaneous modulus.

Samples

Skeletally mature animals

Right and left joints

Visually normal articular surfaces:

- Tibial plateau
- Femoral condyles

Camera-registration system

Articular surfaces were attached to a testing chamber filled with PBS and equipped with a camera-registration system.

A position grid was superimposed on the image of the sample.

Pixels were converted into metric coordinates for the automated surface mapping.

### Automated Indentation

At each position, a perpendicular indentation was performed by simultaneously moving the 3 displacement components (motorized stages) based on the surface orientation and the resulting force is measured with a spherical indenter ( $r=0.5\text{mm}$ ) placed on a multiaxial load cell.

### Automated Thickness Measurement

The spherical indenter was replaced with a Needle probe (26G).

The thickness was obtained by penetrating the cartilage surface down to the subchondral interface.

The Cartilage surface corresponded to the position where the force started to increase, the subchondral interface where the force increased steeply and the vertical thickness was the difference.

Thickness = Vertical thickness x cosine (surface orientation)

### Extraction of the Instantaneous Modulus

The Instantaneous Modulus at each position was obtained by fitting the load-displacement curve to an elastic model in indentation using the measured thickness.

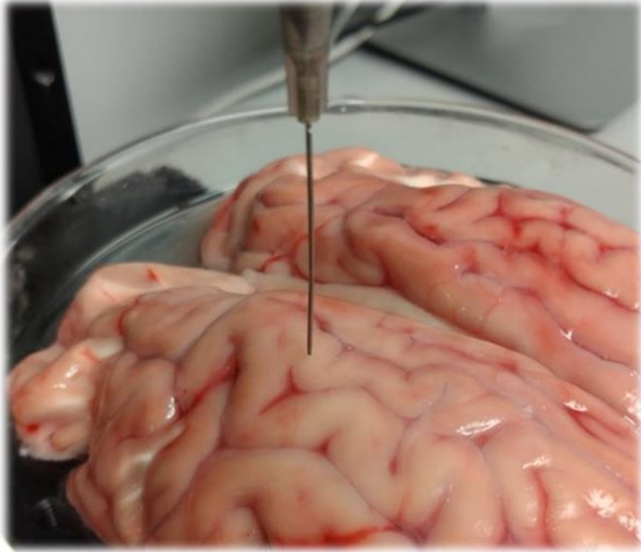
### Results

Spatial distribution of thickness and instantaneous modulus reveals a large variation within the medial and lateral projections of the femoral condyle and tibial plateau. This trend can be observed for all three species. The cartilage is thinner and stiffer in regions covered by the meniscus while a thicker and softer cartilage is observed over the rest of the surface.

Measured thickness agrees with those reported in the literature. The measured instantaneous modulus mappings show similar distribution patterns than those previously observed for the stifle joints of larger species, with stiffer cartilage in the region covered by the meniscus, suggesting a dependence with weight bearing and kinematics.

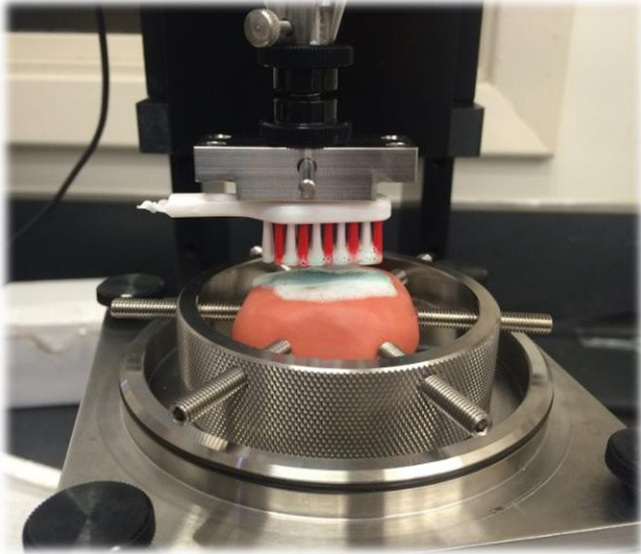
### Conclusion

Cartilage thickness and instantaneous modulus can vary by a factor up to 10 over a distance of only 5% of the total articular surface width. These thickness and modulus maps clearly show that any difference between treated and non-treated cartilage could be confounded with the natural topographic variability rather than due to the treatment itself. By considering the spatial distribution of cartilage properties when choosing control and treated sites, the effects of treatment may be more easily discerned.



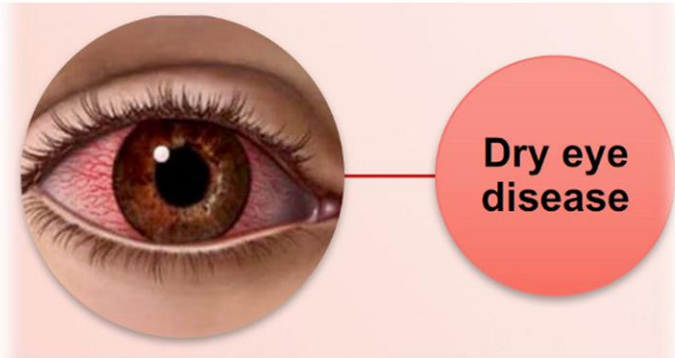
# TESTING OF A BRAIN

Feasibility tests were performed to verify the Mach-1's ability to measure penetration on a brain specimen. Varying needle gauges were used on a veal brain specimen while measuring force with a 50g load cell. The results showed that the 50g load cell was able to capture the varying forces involved.



# TOOTHPASTE TESTING

The Mach-1 can be used to simulate teeth brushing with a controlled offset of pressure on the brush and controlled horizontal brushing movement. In this case, a Mach-1 v500cs was used to produce a mechanical shear force. This method could allow for wear testing alongside the "Find Contact" function in Mach-1 Motion before and after the brushing cycle. A change in height due to constant wear could then be determined quantitatively. A liquid bath could also be used in further testing to better simulate a physiological environment.



# INNOVATIVE FRICTION TESTING ON CONTACT

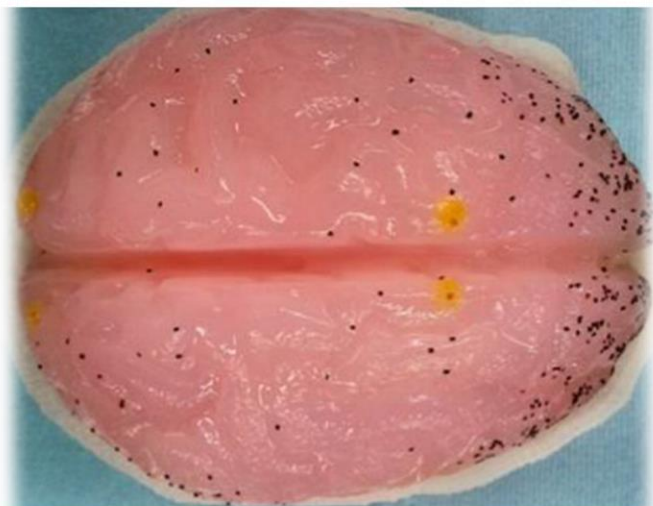
There are over 140 million contact lens wearers worldwide. However, 50% of those report dry eye symptoms. These symptoms are mostly due to friction between the ocular surface and the eyelid during blinking and are exacerbated with contact lens use. Indeed, friction is the strongest indicator of contact lens comfort, although, there is no industry standard for in vitro evaluation of friction in the contact lens industry.

Furthermore, researchers have recently discovered a lubricating glycoprotein at the ocular surface: Proteoglycan 4 (PRG4, or lubricin). PRG4 functions as a boundary lubricant and appears to reduce friction between human eyelids and commercial contact lens. The abundant expression of full-length recombinant human PRG4 (rhPRG4) has been possible with recent technological advances. In a clinical trial, rhPRG4 has shown to produce significant improvement in signs and symptoms of dry eye disease compared to sodium hyaluronate (HA). This is why researchers A.C.Y Chan and Dr. Tannin Schmidt at University of Calgary were interested in investigating: How do different lens types, lubricants and lens incubation times affect rhPRG4 lubrication? They had the goal to understand which commercial lenses are compatible with rhPRG4 for friction reduction as a first step for potential clinical use.

However, this study involved a great challenge, namely that of mimicking the blinking of an eye using a mechanical tester to obtain the kinetic friction coefficient. The researchers turned to the Mach-1 mechanical tester from Biomomentum to perform friction test on curved surface. The Mach-1 is a modular testing machine where a multi-axial load cell (6 degree-of-freedom load/torque) and 3 stages (vertical and horizontals) could be installed. Engineers at Biomomentum worked together with the researchers to develop an algorithm allowing the synchronization of multiple stages to offer the sliding of an eyelid on a contact lens. The kinetic friction coefficient was calculated dividing the shear forces (tangential forces) by the normal force obtained through the multi-axial load cell. The test was performed in PBS solution using a sliding path of  $\pm 10^\circ$  at a sliding velocity of 0.3 mm/s. Two test sequences were performed, a soak test (overnight cleaning solution) and an eye drop test (eye drop solution).

The researchers found that PRG4 may be useful as a friction reducing lubricant (either as an eye drop solution or as an overnight cleaning solution) on specific silicone hydrogel contact lenses with potential improvement of in vivo contact lens comfort. This study has the potential to understand the function and properties of rhPRG4 and thus, initiate the commercialization of rhPRG4 for treatment of dry eye through improved comfort.

This text is based on: Chan A. and Schmidt T. Investigating the effect of recombinant human proteoglycan 4 on the kinetic coefficient of friction of commercial contact lenses. 19th International Society for Contact Lens Research, Stevenson, WA, USA, poster presentation, 13-18 August 2017.



# INNOVATIVE FRICTION TESTING ON CONTACT

One of the most important roles of medical school is giving doctors hands-on training with the tissues they will work with over their career. No one wants to be their surgeon's first time with a brain. But getting enough materials to train everyone can be expensive and ethically challenging, especially when it comes to the brain.

To get past this resource challenge, medical schools have tuned in to using synthetic brains to give students the feel of the real thing. But making a brain is hard, and most of these synthetics just don't match the physical characteristics of real brains. For instance, a real brain responds differently to varying pressure levels and speeds of movement, but most training "brains" don't display these nuances. These non-linear responses are key to giving a budding brain surgeon an authentic training experience, and the available materials can't live up to the real thing. That's why researchers Antonio E. Forte and Daniele Dini at Imperial College London set out to break the mold by creating a synthetic brain that accurately mimics the essential physical properties of the brain and can be cheaply and easily produced.

They turned to the Mach-1 mechanical tester from Biomomentum to test varying combinations of materials for essential brain-like properties like how they compress with varying pressure and speeds; the speed of recovery after injury; their response to shaking; and, of course, their response to incision. The Mach-1 was used to compare these essential surgical properties of the synthetic material combinations to pig brains, which have nearly identical properties to human brain. This fundamental research was published in the journal of Materials and Design.

The researchers found that combining two gels, Polyvinyl Alcohol (PVA) and Phytigel (PHY), creates a material with very similar physical properties to human brain tissue. They created a life-size version of the brain that floats on cerebrospinal fluid, maintains all its brain-like properties, and could easily be used in a medical school. This innovation could provide drastically needed changes to medical school training, upping the talent level of novice brain surgeons worldwide.

Inspired from Forte AE, Galvan S, Manieri F, y Baena FR and Dini D. A composite hydrogel for brain tissue phantoms. *Materials & Design*, 112, 227-238 (2016)